Australian Government
Department of Defence
Defence Science and
Technology Organisation

Preliminary Report on Pulse Compression Waveforms and their Application to Waveform Agility

Graeme Nash

Weapons Systems Division
Systems Sciences Laboratory

DSTO-TR-1631

ABSTRACT

Pulse Doppler radars predominantly transmit the same pulse compression waveform pulse to pulse. This produces good Doppler performance in a jammer free environment. But in a jammer environment the transmitted pulses can be captured by a digital RF memory (DRFM) and retransmitted creating false targets. By introducing pulse to pulse waveform agility the effectiveness of the jammer can be greatly reduced.

Published by

DSTO Systems Sciences Laboratory
PO Box 1500
Edinburgh South Australia 5111 Australia

Telephone: (08) 8259 5555
Fax: (08) 8259 6567

AR-013-212
October 2004

APPROVED FOR PUBLIC RELEASE

Preliminary Report on Pulse Compression Waveforms and their Application to Waveform Agility

Executive Summary

Pulse Doppler radars are widely used in the Australian Defence Force (ADF) to detect targets in the air, on the sea and on land. Radars that repeatedly transmit the same waveform are susceptible to jammers that have digital radiofrequency memories (DRFM) which can record the waveform and retransmit it causing false targets in the radar in such a way that true targets are not correctly detected. This report investigates the effectiveness of waveform agility (i.e. varying the waveform from pulse to pulse in an unpredictable way) for overcoming the jamming.

Possible applications of waveform agility to the ADF include all future pulse Doppler radars that require electronic protection (EP). Radar systems presently in service with the ADF would require hardware changes to implement waveform agility which would be very costly, but for future radar systems waveform agility could probably be implemented with software changes only.

Authors

Dr Graeme Nash
Weapons Systems Division

Dr Graeme Nash has a B.ENG (S.A.I.T 1987), and a PhD (Uni of S.A. 1995). Graeme is currently working in the field of radar signal processing.

Contents

Glossary

BBC	binary barker code
BC	binary code
BoBC	Barker on Barker code
CMC	constant magnitude code
CW	continuous wave
DRFM	digital radio frequency memory
EP	electronic protection
FC	Frank code
ISL	integrated sidelobe level
MPCF	mismatched pulse compression filter
PBC	polyphase Barker code
PC	polyphase code
PJL	peak jammer level
PNC	pseudo noise code
PSL	peak sidelobe level
PPC	perfect periodic code
PRC	primitive root code
PRF	pulse repetition frequency
QRC	quadratic residue code
SNR	signal to noise ratio
TC	ternary code

1. Introduction

Pulse Doppler radar systems are widely used to detect targets. Radar systems that repeatedly transmit the same waveform are susceptible to jammers that have digital RF memories (DRFM), which can record the waveform and retransmit it causing false targets in the radar in such a way that true targets are not correctly detected. This report investigates the effectiveness of waveform agility (i.e. varying the waveform from pulse to pulse in an unpredictable way) for overcoming the jamming.

The effectiveness of waveform agility is investigated by determining the peak sidelobe level (PSL) for the target-only case and by determining the peak jammer level (PJL) for a single jammer case, for various pulse trains including chirps, Frank codes, Barker codes, Barker on Barker codes and optimised codes.

Possible applications of waveform agility include all future pulse Doppler radars that require electronic protection (EP). Radar systems presently in service would require hardware changes to implement waveform agility, which would be very costly, but for future radar systems waveform agility could probably be implemented with software changes only.

2. Pulse Compression Waveforms

To collect a range profile a radar system transmits a pulse and then samples the received signal. Consider a transmitted pulse with bandwidth B, centred at a carrier frequency of f_0, with a time duration of T where [1],

$$T = N\tau$$

and

$$\tau = \frac{1}{B}$$

and N is an integer. Assuming quadrature sampling the waveform can be modelled as a sequence of complex subpulses ,

$$a_0, a_{1,}, \ldots, a_{N-1}$$

with a sampling interval of τ multipled by the carrier signal,

$$s(t) = \exp(\, j2\pi f_0 t)$$

If the pulse consists of a simple sinusoid (in which case the sequence is a single sample) then the range resolution ΔR is directly proportional to the time duration T of the pulse, in fact,

$$\Delta R = \frac{cT}{2}$$

where c is the speed of light. Therefore by reducing the pulse length T the range resolution ΔR is improved, but this decreases the signal to noise ratio (SNR) because radar systems have a limit on the peak power they can transmit.

For a general pulse the range resolution ΔR is [1],

$$\Delta R = \frac{c}{2B}$$

where B is the bandwidth of the pulse. By transmitting a coded pulse such as a chirp the range resolution ΔR and the pulse duration T (and therefore the SNR) can be independently controlled.

The use of coded waveforms has an additional electronic protection (EP) benefit because it reduces the effectiveness of jamming by an adversary who doesn't know the pulse waveform. This is because the jamming signal will not be increased by the coherent processing gain, whereas the return from a target will be increased by the coherent processing gain.

The main disadvantage of pulse compression waveforms is the appearance of sidelobes. For a range Doppler radar these always occur for code sequences of length greater than one and are determined by calculating the autocorrelation series of the code sequence. For the case of transmitting a single pulse (as in range Doppler radar) the autocorrelation series is,

$$\chi_l = \sum_{n=l}^{N-1} a_n a_{n-l}^*, l = 0,1,2,\ldots,N-1,$$

where * indicates the complex conjugate. The code sequence can be oversampled by repeating each value a certain number of times to determine the autocorrelation series for ranges that are not integral multiples of the range resolution ΔR. Note that the case where the range R is an integral multiple of ΔR is called the bin centred case, otherwise it is called the non-bin centred case.

For a continuous wave (CW) radar it is possible to find sequences for which the autocorrelation series is zero everywhere except at zero lag and therefore there are no sidelobes. These are termed perfect periodic codes (PPC) [2]. CW radars are not suitable for situations where the unambiguous range of detected targets is required because CW radars cannot determine the unambiguous range of detected targets.

Due to practical limitations of radar systems it is often desirable or even necessary to put restrictions on the values of the code sequence. The peak power of radar systems is limited and so setting all the code sequence values to a magnitude of unity will maximise the power transmitted and therefore the SNR. These codes are called constant magnitude codes (CMC). Some radars are capable of only generating a fixed number of phase shifts, such as two phases (binary codes (BC)), three phases (ternary codes (TC)), etc. These codes are collectively termed polyphase codes (PC). These amplitude and phase restrictions can result in worse sidelobe performance.

A further complication of the use of pulse compression waveforms is the performance degradation caused by the Doppler shift f_d induced by any target that is moving with respect to the radar. Doppler shifting causes the reflected signal to be a modulation of the transmitted signal with the Doppler frequency f_d resulting in a mismatch with the receiver. This can be studied using the radar ambiguity function $\phi(l, f_R)$, defined here as [1],

$$\phi(l, f_R) = \sum_{n=l}^{N-1} a_n a_{n-l}^* \exp(j2\pi f_R n) \quad (1)$$

where $f_R = \frac{f_d}{B}$ is the relative Doppler frequency. If the Doppler frequency f_d results in too much degradation then multiple pulse compression filters will be required with each filter matched to a different Doppler frequency so that each filter has a sufficiently small Doppler offset. Note that the effect of the Doppler frequency f_d can be compensated for if it is known. For the example of an aircraft detecting ships, the affect of the motion of the aircraft can be compensated for leaving only the Doppler due to the unknown ship motion [1].

2.1 Sampled Chirp Codes

2.1.1 Linear Chirps

A linear chirp is a signal with a quadratic phase so that its instantaneous frequency is a linear function of time. Sweeping the instantaneous frequency over the required bandwidth B results in the chirp having a bandwidth approximately equal to B. A continuous linear chirp [3] when sampled can be represented by the sequence,

$$a_n = \exp(j\frac{\pi n^2}{N}), n = 0,1,2,\ldots,N-1$$

Recalling that the time interval $\tau = \frac{1}{B}$ we see that the instantaneous frequency sweeps from $-\frac{B}{2}$ to $+\frac{B}{2}$. The code sequence is a CMC.

The P3 code is [4],

$$a_n = \exp(j\frac{\pi n^2}{N}), n = 0,1,2,\ldots,N-1$$

which is the same as the definition of the sampled linear chirp. The P4 code is [4],

$$a_n = \exp(j(\frac{\pi n^2}{N} + \pi n), n = 0,1,2,\ldots,N-1$$

which only differs from the sampled linear chirp by a linear frequency term and so will still have the same magnitude autocorrelation series. So we shall consider only sampled chirps, but the sidelobe levels found will also be applicable to the P3 and P4 codes.

Figure 1 shows a sampled chirp code and its autocorrelation series from which we see that the PSL is approximately 26 dB below the mainlobe. Figure 2 shows the radar ambiguity function for the same waveform. This is a good radar ambiguity function because there is a sharp response and low sidelobes over the whole relative Doppler frequency f_R extent. The location of the peak moves a bit in range which means that the Doppler is causing a range error.

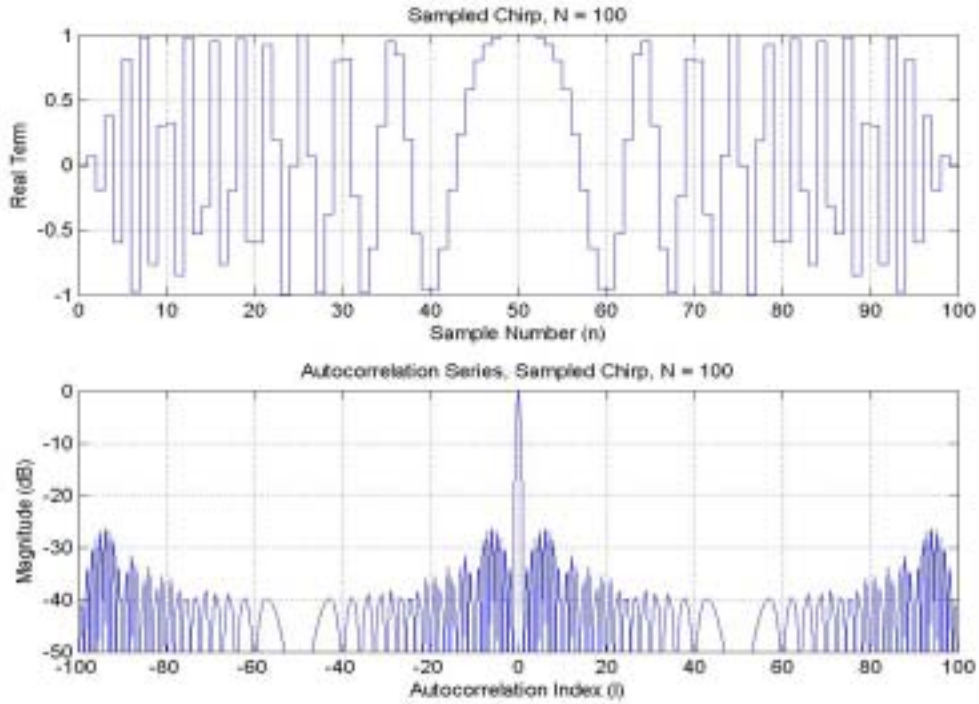

Figure 1. A Linear Sampled Chirp and its Response Function

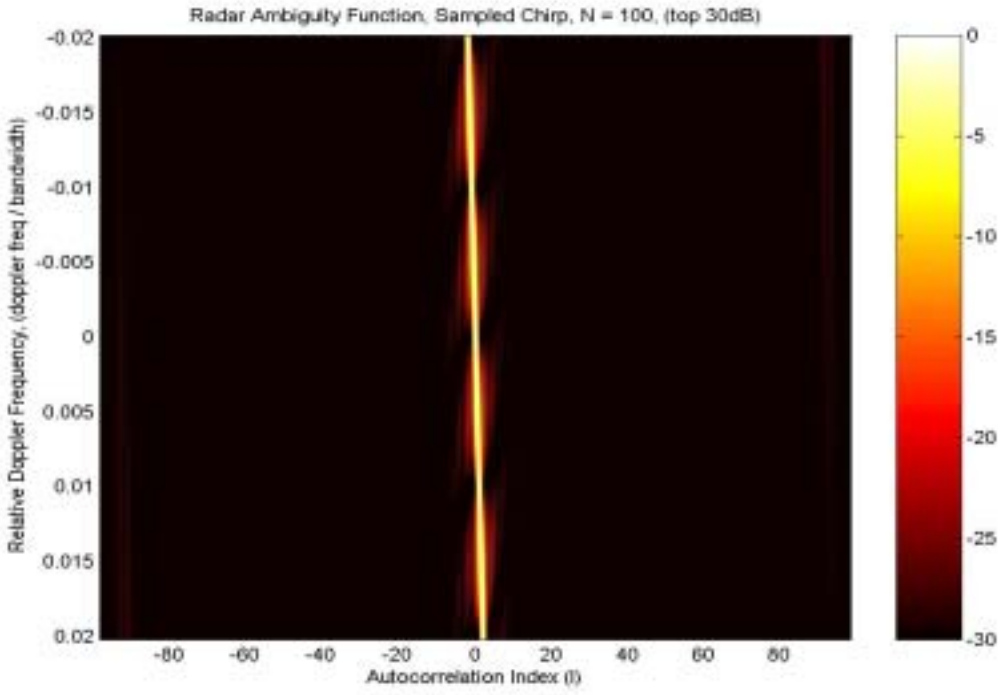

Figure 2. Radar Ambiguity Function for a Sampled Linear Chirp

2.1.2 Linear Chirps with Windowing

To reduce the sidelobe levels that result from linear chirps a weighting function (such as Hann, Hamming etc.) [3] can be applied to a linear chirp in the frequency domain both to the transmitted waveform and the matched filter waveform. This will lower the sidelobe levels at the cost of increasing the width of the mainlobe and so reducing the range resolution. The weighting will also reduce the power transmitted and therefore the SNR. Figure 3 shows a sampled linear chirp weighted with a Hamming window. The weighting applied in the frequency domain leads to a weighting in the time domain because of the time frequency correlation that linear chirp waveforms have. The application of the weighting has changed the structure of the sidelobes and reduced the PSL down to 32 dB below the mainlobe (see Figure 3). The radar ambiguity function shown in Figure 4 is very similar to the non-windowed case, except that the peak is wider.

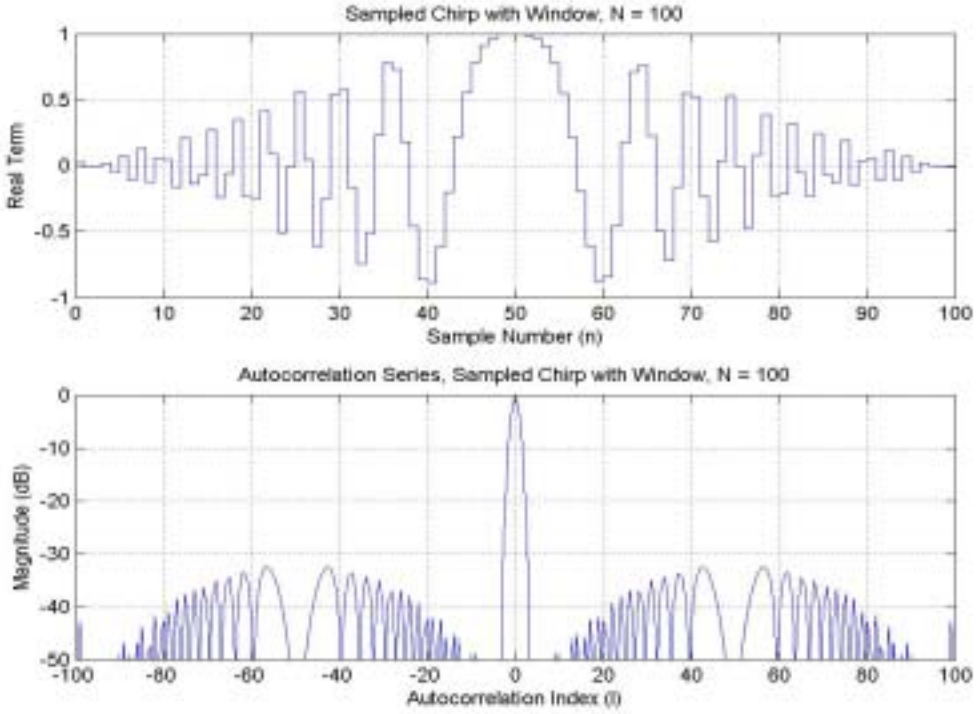

Figure 3. A Linear Sampled Chirp with a Hamming Window and its Response Function

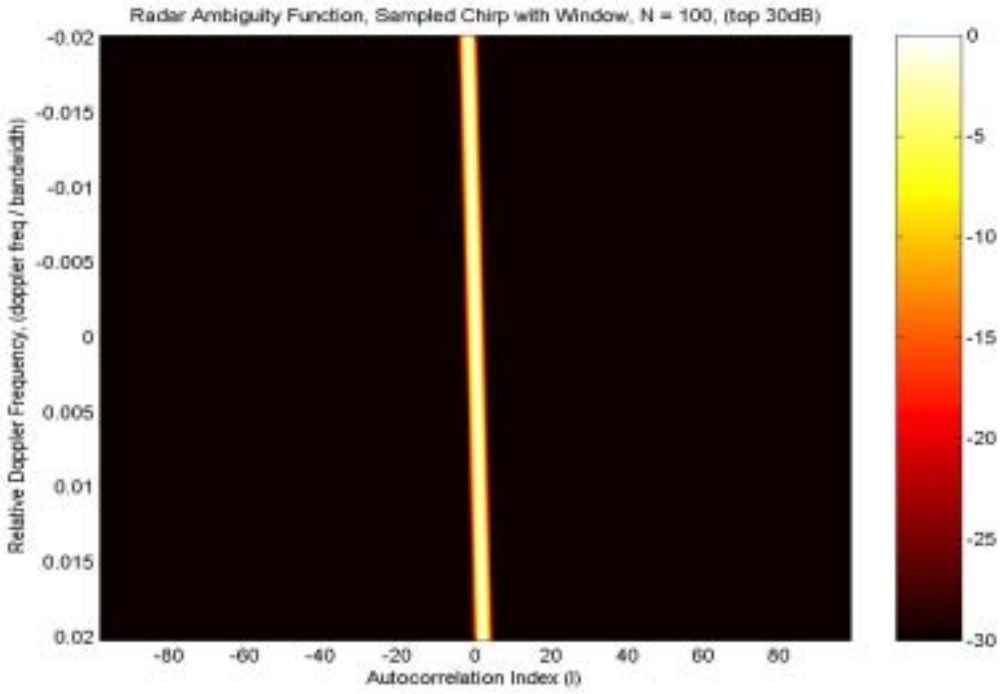

Figure 4. Radar Ambiguity Function for a Sampled Chirp with Hamming Window

2.1.3 Non-Linear Chirps

To achieve weighting in the frequency domain without a reduction in the power transmitted (and therefore the SNR) a non-linear chirp can be used. Using the procedure by Felhauer [7], a non-linear chirp can be generated by the following process.

From [7] a waveform with constant magnitude has the group time delay function $T(f)$ of the form,

$$T(f) = -\int G(f)^2 df$$

where $G(f)^2$ is the envelope of the waveform in the frequency domain, and therefore $G(f)^2$ may be set to a standard windowing function. The instantaneous frequency $f_i(t)$ of the waveform is given by,

$$f_i(t) = T^{-1}(f)$$

and so the phase of the waveform $\varphi(t)$ is,

$$\varphi(t) = \int 2\pi T^{-1}(f) df .$$

The weighting function used by Felhauer [7] is,

$$G(f)^2 = \left(k + (1-k)\cos^q\left(\pi f / B \right) \right), |f| \le \frac{B}{2}$$

with $q = 4$ and $k = 0.015$. The continuous angle function $\varphi(t)$ is then sampled to produce N samples. That is,

$$a_n = \exp\left(j2\pi\varphi\left(\frac{(n-N)T}{2N} \right) \right), n = 0,1,2,\ldots,N-1.$$

For general values of q and k some of the above integrals have no closed form solution and so are solved numerically.

For $q = 4$ and $k = 0.015$ the integral for the group time delay function $T(f)$ was estimated numerically. The instantaneous frequency $f_i(t)$ was then formed by interpolation of the group time delay function $T(f)$ onto a regular grid. Then the integral for $\varphi(t)$ was estimated numerically and then interpolated to get the N samples $a_0, a_1, \ldots, a_{N-1}$.

From Figure 5 it is clear that the non-linear sampled chirp has low sidelobes with PSL = -38 dB. Figure 6 shows its radar ambiguity function which has no sidelobes above –30dB and the peak moves slightly with dopper frequency but does not distort.

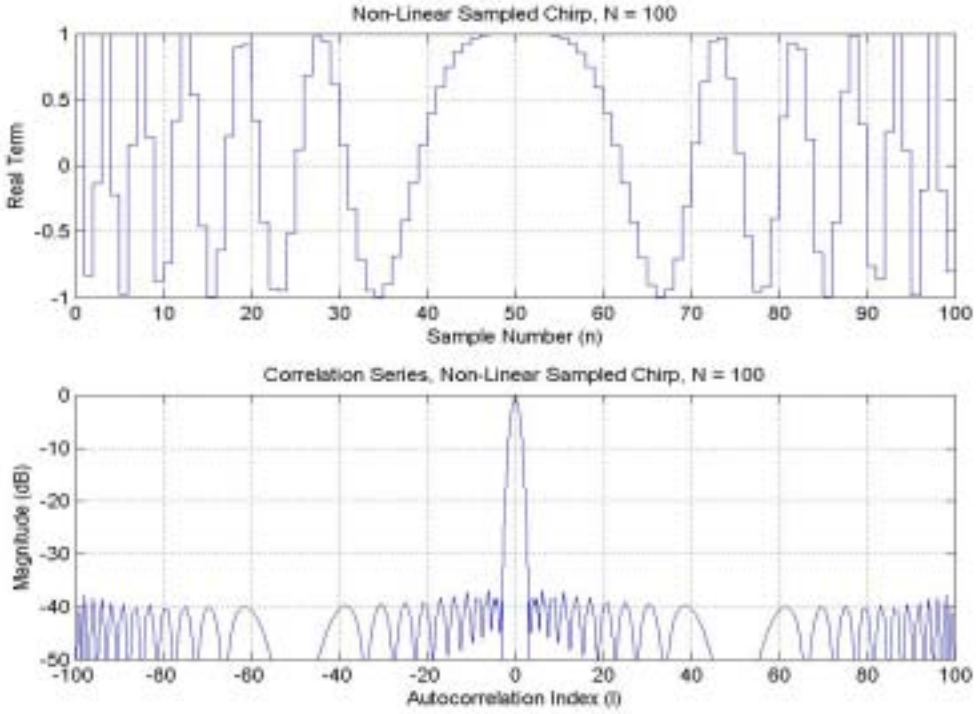

Figure 5. A Non-Linear Sampled Chirp Code and its Response Function

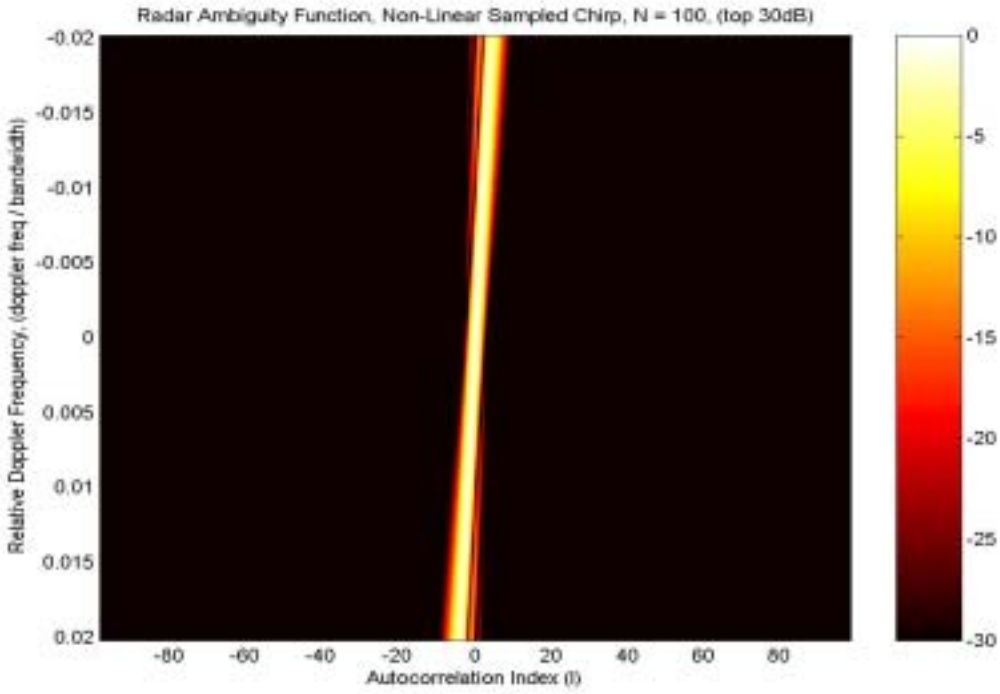

Figure 6. Radar Ambiguity Function for a Non-Linear Sampled Chirp

2.2 Frank Codes

Frank codes [4] are a type of sampled chirp, but whereas the instantaneous frequency in a sampled chirp rises steadily, for a Frank code (FC) it rises only once every $\sqrt{N}$ (where N is chosen so that $\sqrt{N}$ is an integer). Frank codes are defined as [4],

$$a_n = \exp(j2\pi \frac{rkm}{M})$$

where,

$$m = \text{int}(n/M)$$
$$k = n - mM$$

r is chosen to be co-prime with M (i.e. no common factors between r and M), $1 \le r < M$ and the integer $M = \sqrt{N}$. Therefore Frank codes are CMC and PC, but the number of phases must be the square root of the code sequence length N. Frank codes are also PPCs. Figure 7 shows a Frank code and it's response. We see that its PSL is –30 dB below the mainlobe. Figure 8 shows the radar ambiguity function for a Frank code. We see that the main peak splits into two peaks at times and the sidelobes also vary quite a lot, which will result in a high PSL for some relative Doppler frequency f_R values.

Note that the P1 code is the same as the Frank code and that the P2 code is a Frank code with the first and second halves swapped around [8].

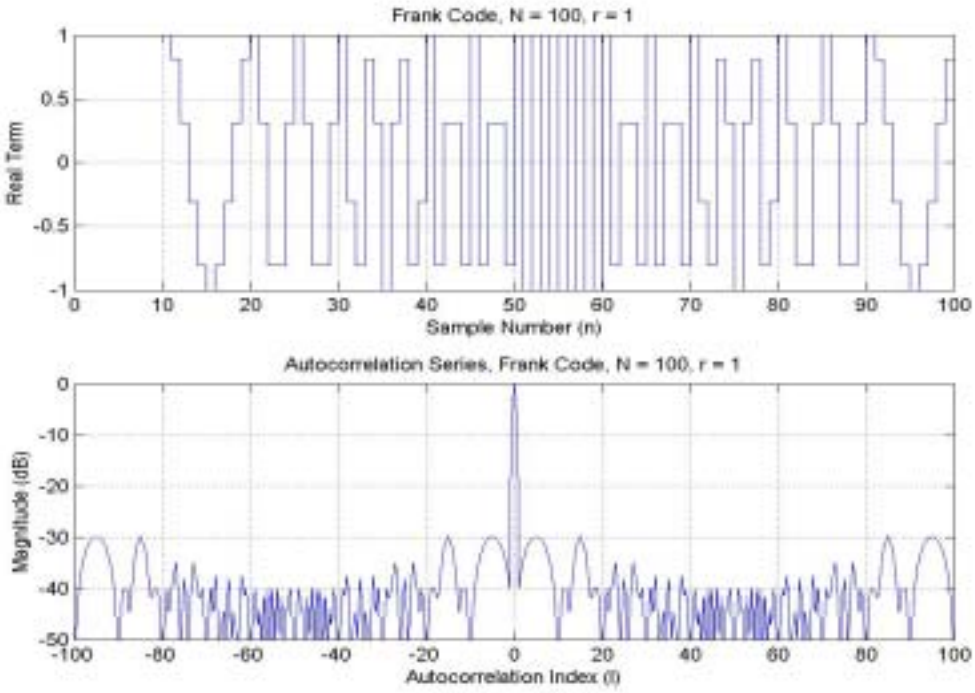

Figure 7. A Frank Code and its Response Function

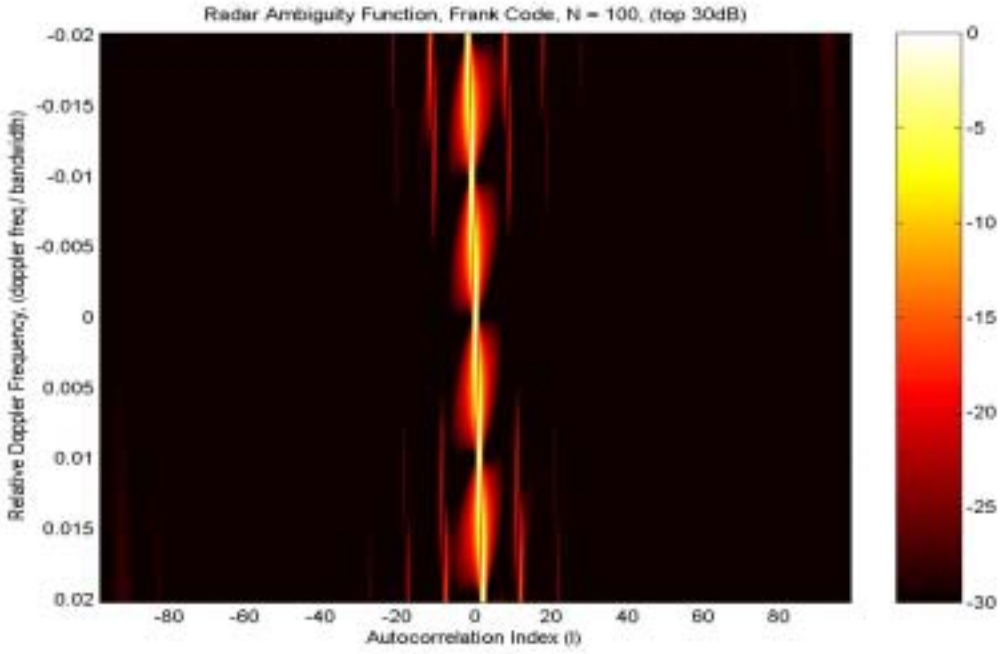

Figure 8. Radar Ambiguity Function for a Frank Code

2.3 Barker Codes

The aperiodic autocorrelation series of a CMC will always end in a term that has unit magnitude (since the elements of a CMC are all unit magnitude) and so the best possible sidelobe response is to have all sidelobes less than or equal to one. These codes have been termed binary Barker codes (BBC) [10] for the case where only two phases are allowed and polyphase Barker codes (PBC) [10] where the number of phases allowed is more than two. There is no known equation for generating BBCs or PBCs and so they must be searched for numerically.

2.3.1 Binary Barker Codes

BBCs have been found for the cases of code length $N = 2,3,4,5,7,11,13$ [10]. Codes may exist for other values of N, but much searching by numerous researchers has failed to find any more. An example of a length 5 BBC is,

$$a_n = \{1,1,1,-1,1\}$$

and an example of a length 13 BBC is,

$$a_n = \{1,1,1,1,1,-1,-1,1,1,-1,1,-1,1\}$$

Figure 9 shows a BBC of length 13, which we see has a PSL of –22 dB below the mainlobe. Table 1 gives all the known BBCs including codes that are the inverse or the reverse of another BBC (These were generated by the Author using an exhaustive search). Figure 10 shows the radar ambiguity function for a BBC of length 13. We see that the width of the mainlobe varies with the relative Doppler frequency f_R and that the sidelobes also vary to some degree.

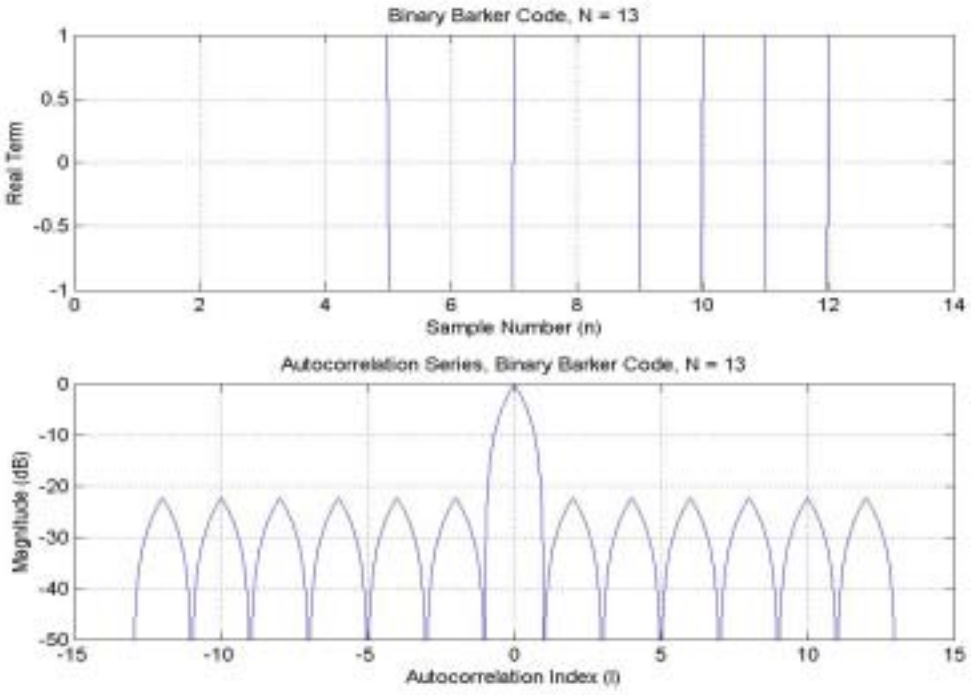

Figure 9. A Binary Barker code and its Response Function

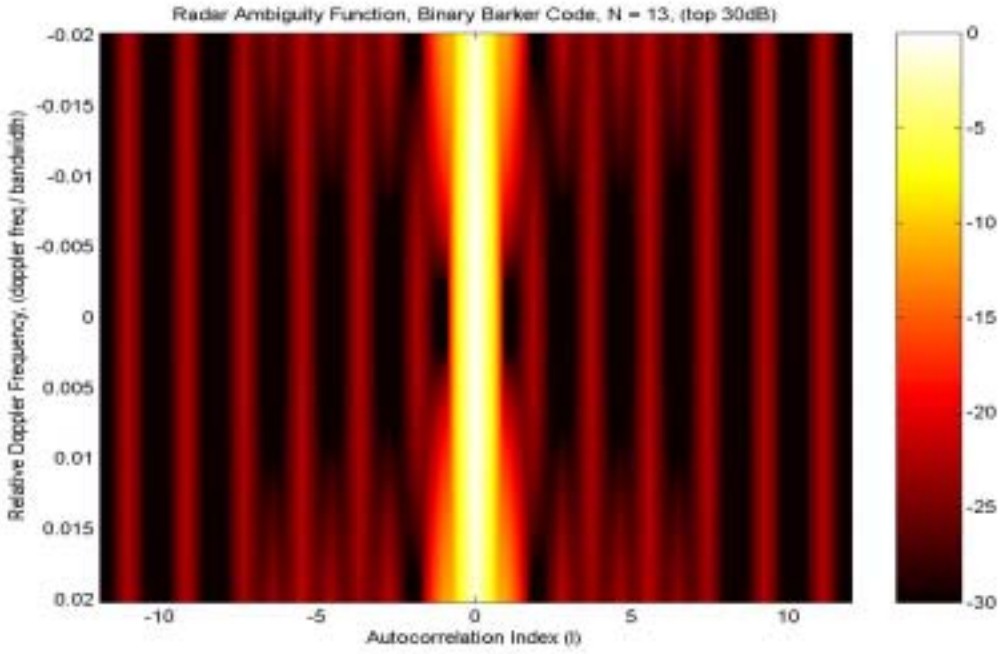

Figure 10. Radar Ambiguity Function for a Binary Barker Code of Length N = 13

Table 1. All the Known Binary Barker Codes

Code Length N	Binary Barker Codes a_n
2	{1,1}, {1,-1}, {-1,1}, {-1,-1}
3	{1,1,-1}, {1,-1,-1}, {-1,1,1}, {-1,-1,1}
4	{1,1,1,-1}, {1,1,-1,1}, {1,-1,1,1}, {1,-1,-1,-1}, {-1,1,-1,-1}, {-1,-1,1,-1}, {-1,-1,-1,1}
5	{1,1,1,-1,1}, {1,-1,1,1,1}, {-1,1-1,-1,-1}, {-1,-1,-1,1,-1}
7	{1,1,1,-1,-1,1,-1}, {1,-1,1,1,-1,-1,-1} {-1,1,-1,-1,1,1,1}, {-1,-1,-1,1,1,-1,1}
11	{1,1,1,-1,-1,-1,1,-1,-1,1,-1}, {1,-1,1,1,-1,1,1,1,-1,-1,-1} {-1,1,-1,-1,1,-1,-1,-1,1,1,1} {-1,-1,-1,1,1,1,-1,1,1,-1,1}
13	{1,1,1,1,1,-1,-1,1,1,-1,1,-1,1} {1,-1,1,-1,1,1,-1,-1,1,1,1,1,1} {-1,1,-1,1,-1,-1,1,1,-1,-1,-1,-1,-1} {-1,-1,-1,-1,-1,1,1,-1,-1,1,-1,1,-1}

2.3.2 Polyphase Barker Codes

Ternary Barker codes (three phases) have only been found up to $N = 9$, Quarternary Barker codes (four phases) have only been found up to $N = 15$ and Sextic Barker codes (six phases) have only been found up to $N = 13$ [9].

2.3.3 Barker on Barker Codes

Because BBC are fairly short sometimes Barker on Barker codes (BoBC) are used to generate a longer (and therefore higher power) code sequence. This involves modulating one BBC with another BBC. For example a length 5 BBC modulated with the length 13 BBC gives a code of length 65. From Figure 11 we see that the BoBCs have very interesting sidelobe structures, however they also can have very large peak sidelobe levels. In this case the PSL is 13 dB below the mainlobe. Figure 12 shows the radar ambiguity function for a BoBC. We see that the mainlobe and the sidelobes vary in a fairly complicated way with the relative Doppler frequency f_R.

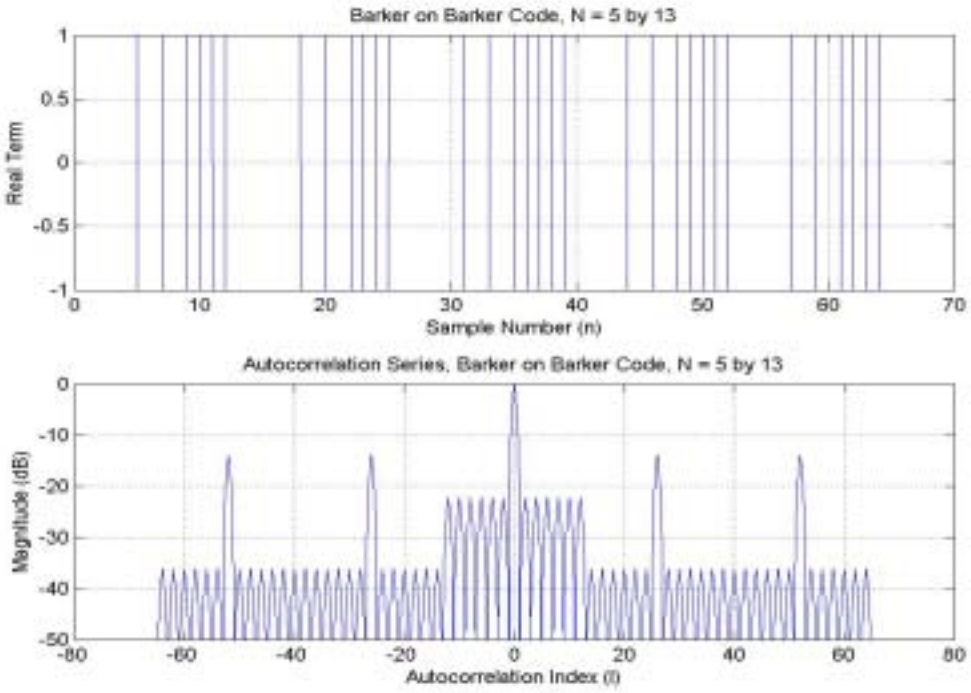

Figure 11. Barker on Barker Code and its Response

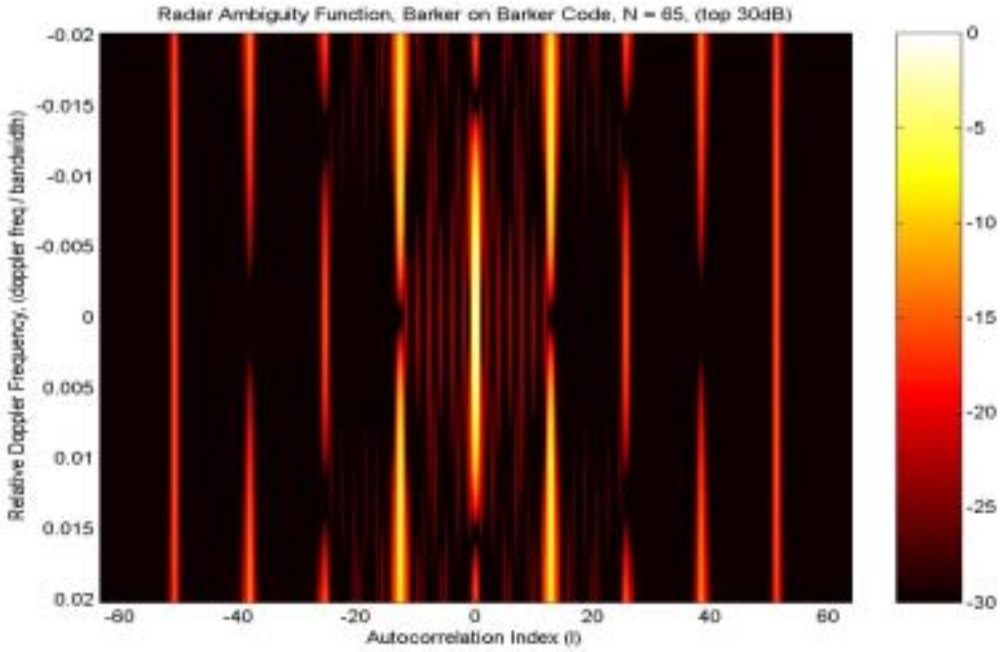

Figure 12. Radar Ambiguity Function for a Barker on Barker Code

2.4 Pseudo Noise Codes

Pseudo Noise Codes (PNC) are maximal length binary codes that are generated using a shift register as shown below in Figure 13 [3].

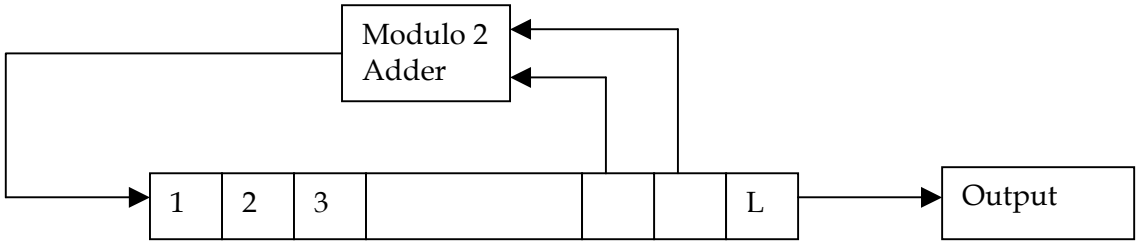

Figure 13. Shift Register used to Generate Pseudo Noise Sequences

When a non-zero initial state is set and suitable feedback is used this will generate a non-repeating code of length $N = 2^L - 1$. Table 2 gives all the feedback stage connections for the number of stages equal to 2 to 9 [11]. For example with 5 stages feeding back bits 3 and 5 into the modulo 2 adder will produce a maximal length code. Similarly feeding back bits 2,3,4 and 5 into the modulo 2 adder will also produce a maximal length code. Figure 14 shows a pseudo noise code for length $N = 127$. We see that the PSL is 21 dB below the mainlobe and that the sidelobes are very unstructured. Figure 15 shows that the mainlobe disappears if $|f_R| \geq 0.005$. Therefore this matched filter could only be used over a relative Doppler frequency extent of –0.005 to +0.005.

Table 2. Pseudo Noise Sequence Feedback Connections for Maximal Length Codes

Number of Stages L	Length of Sequence N	Number of Maximal Sequences	Feedback Stage Connections
2	3	1	{1,2}
3	7	2	{2,3}
4	15	2	{3,4}
5	31	6	{3,5},{2,3,4,5},{1,3,4,5}
6	63	6	{5,6},{1,4,5,6},{2,3,5,6}
7	127	18	{6,7},{4,7},{4,5,6,7}, {2,5,7,6},{2,4,6,7}, {1,4,6,7},{3,4,5,7}, {2,3,4,5,6,7},{1,2,4,5,6,7}

8	255	16	{1,6,7,8},{3,5,7,8}, {2,3,7,8},{4,5,6,8}, {3,5,6,8},{2,5,6,8}, {2,4,5,6,7,8},{1,2,5,6,7,8}
9	511	48	{5,9},{2,7,8,9},{5,6,8,9}, {4,5,8,9},{1,5,8,9},{2,4,8,9}, {4,6,7,9},{2,5,7,9},{3,5,6,9}, {3,5,6,7,8,9},{1,5,6,7,8,9}, {3,4,6,7,8,9},{2,4,6,7,8,9}, {2,3,6,7,8,9},{1,3,6,7,8,9}, {1,2,6,7,8,9},{3,4,5,7,8,9}, {2,4,5,7,8,9},{1,4,5,6,8,9}, {2,3,5,6,8,9},{1,3,5,6,8,9}, {3,4,5,6,7,9},{2,4,5,6,7,9}, {1,3,4,5,6,7,8,9}

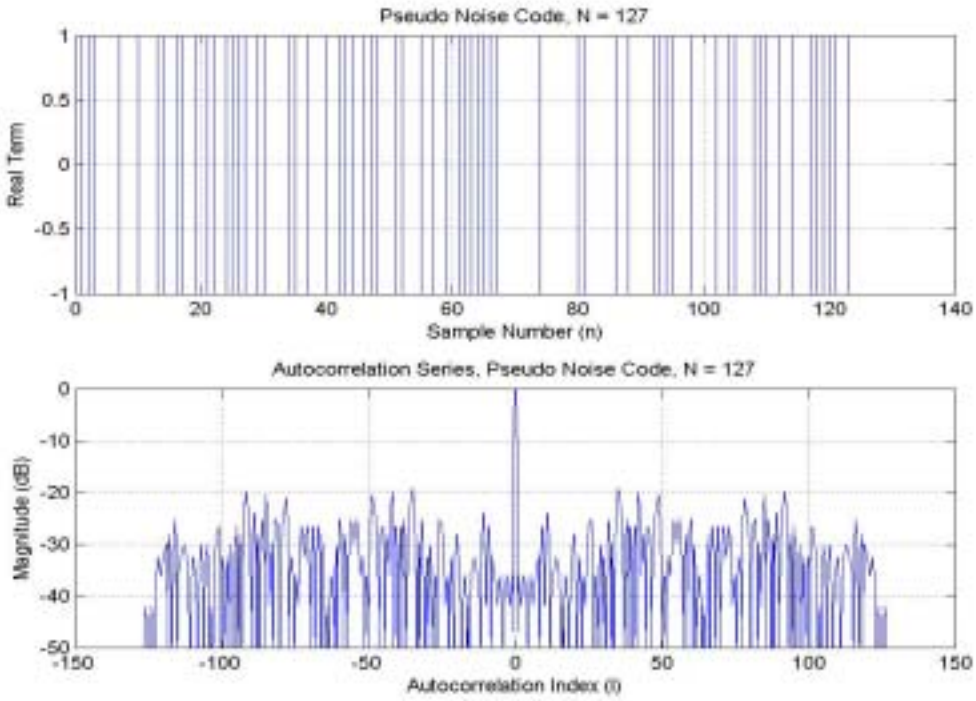

Figure 14. Pseudo Noise Code and its Response

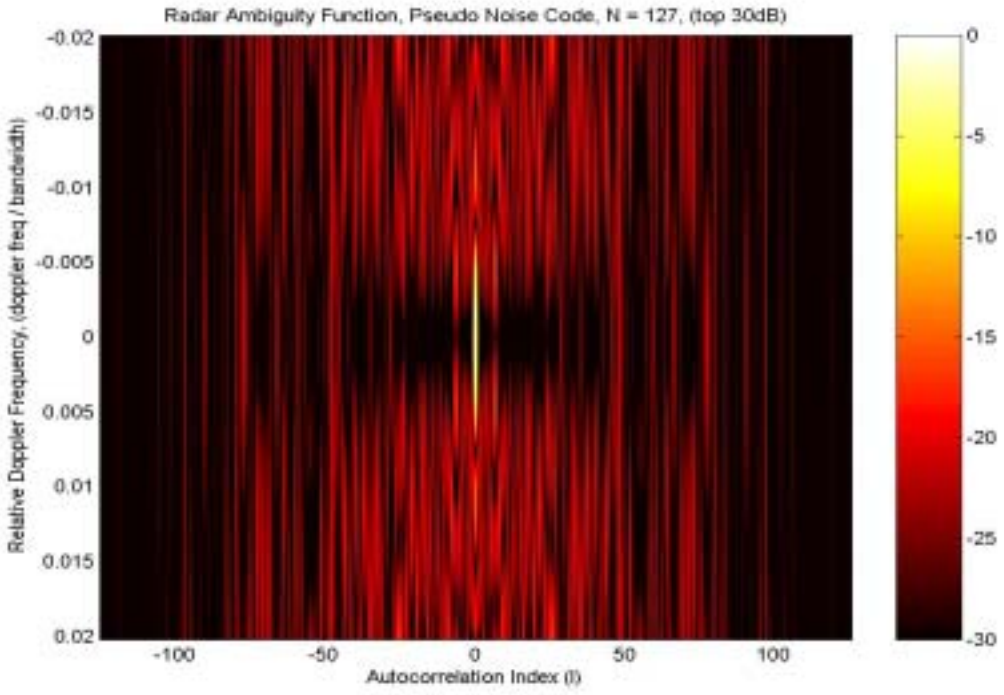

Figure 15. Radar Ambiguity Function for a Pseudo Noise Code

2.5 Miscellaneous Codes

There are other codes that appear in the literature. A couple of them are the primitive root code (PRC) and the quadratic residue code (QRC) [12]. The PRC is defined as,

$$a_n = \exp(j2\pi \frac{\alpha^n}{N+1}), n = 0,1,2,\ldots,N-1$$

where N is chosen such that $N+1$ is a prime number and α is a primitive root of $N+1$. Figure 16 shows an example of a PRC and has a PSL of 12 dB below the peak level. Figure 17 is a plot of the radar ambiguity function which shows that while the mainlobe stays fairly constant the sidelobes vary a bit with relative Doppler frequency f_R. Table 3 lists the number of different primitive roots α available for each valid code length N (These were calculated by the Author).

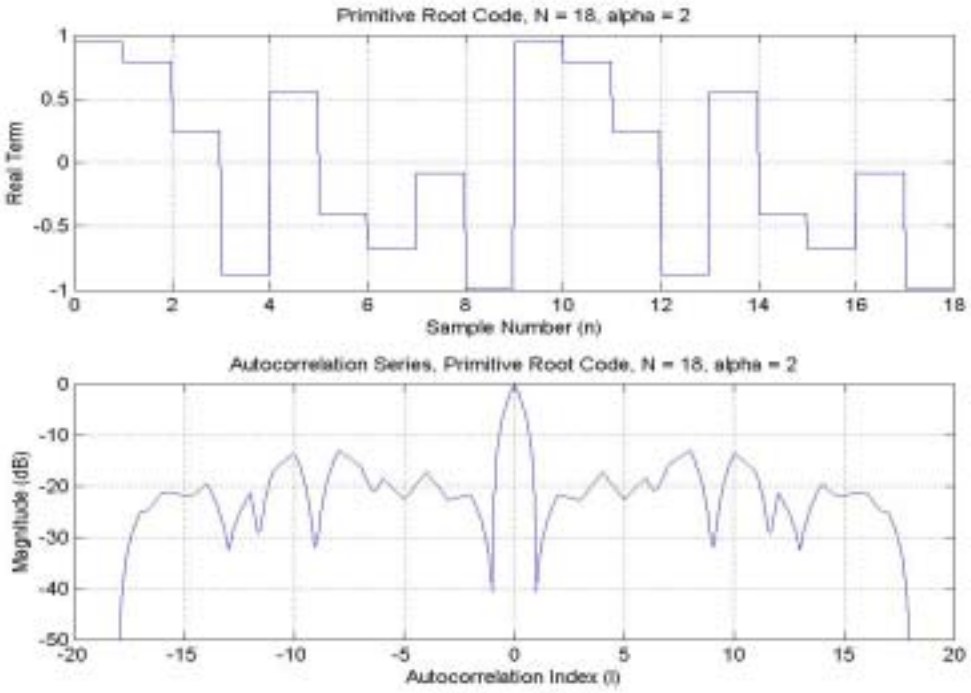

Figure 16. A Primitive Root Code and its Response

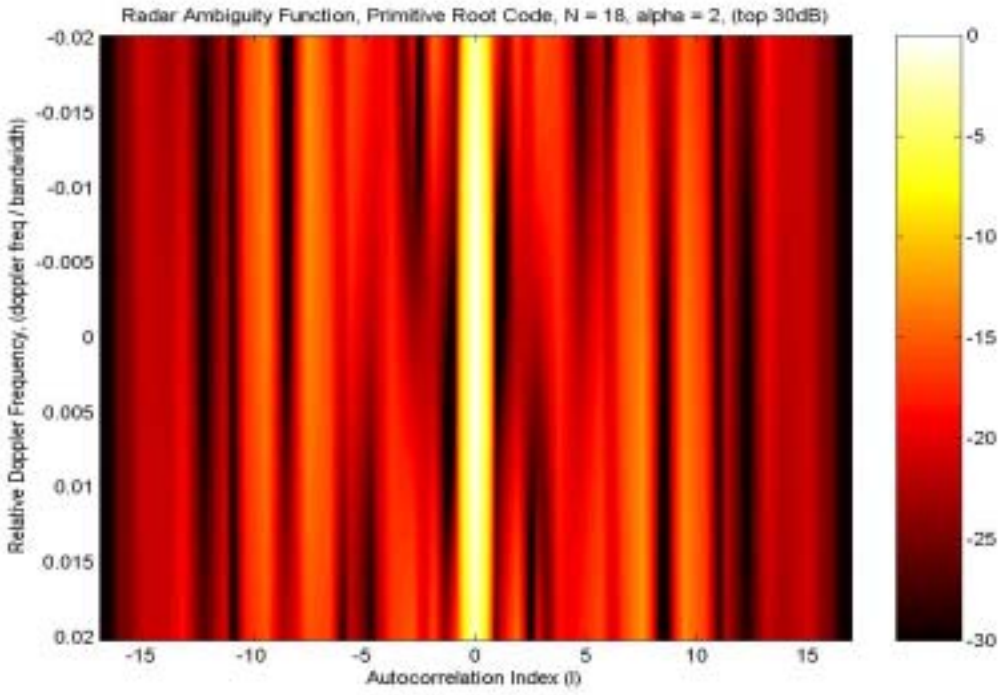

Figure 17. Radar Ambiguity Function for a Primitive Root Code

Table 3. Number of Primitive Roots for Valid Values of Code Length N up to 100

N (Values Valid for Primitive Root Code up to 100)	Number of Primitive Roots of N+1
2	1
4	2
6	2
10	4
12	4
16	8
18	6
22	10
28	12
30	8
36	12
40	16
42	12
46	22
52	24
58	28
60	16
66	20
70	24
72	24
78	24
82	40
88	40
96	32

The QRC is defined as,

$$a_n = (n/N), n = 0,1,2,\ldots,N-1$$

for the case of $N = 4m - 1$ is a prime number for m a positive integer, where (n/N) is the Legendre Symbol which is defined for all n which are not divisible by N [12]. The Legendre Symbol is equal to 1 if n is a quadratic residue of N and –1 otherwise. Note that n is a quadratic residue of N if,

$$z^2 = n(\mathrm{mod}\, N)$$

has a solution for some integer z. Figure 18 shows an example of a QRC and has a PSL of 12 dB below the mainlobe . Figure 19 of the radar ambiguity function shows that the mainlobe fades out if $|f_R| \geq 0.015$, but within this limit both the main peak and the sidelobes are fairly constant.

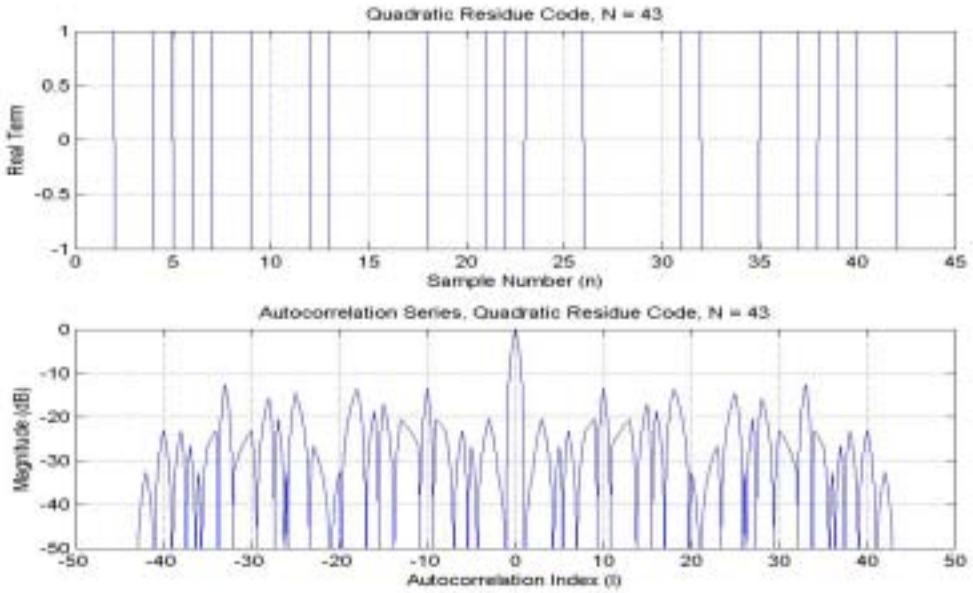

Figure 18. A Quadratic Residue Code and its Response

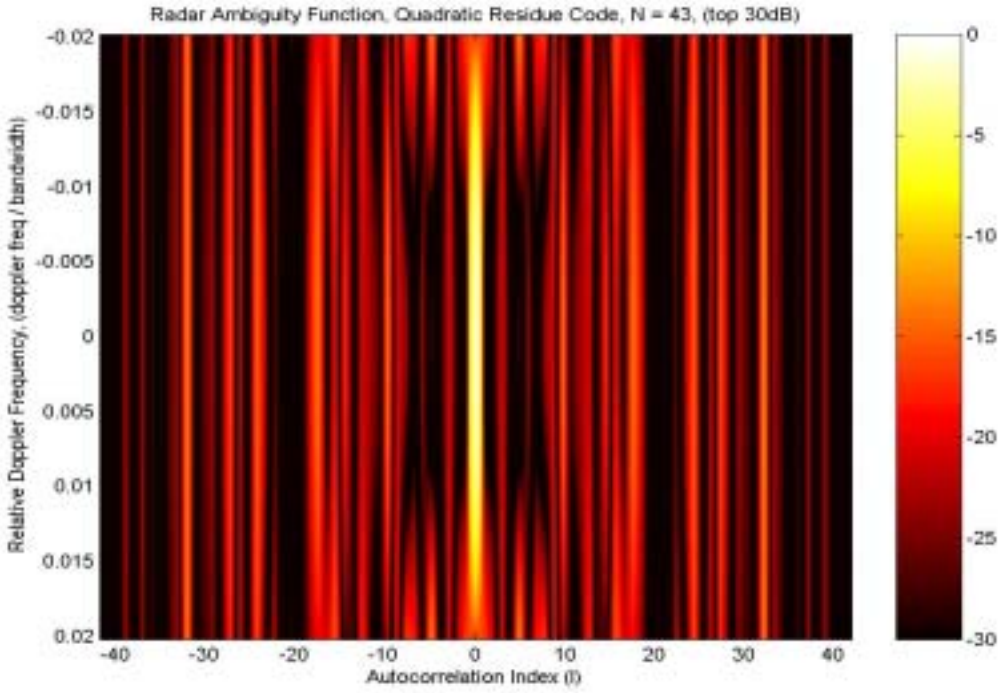

Figure 19. Radar Ambiguity Function for a Quadratic Residue Code

2.6 Codes Formed by the Optimisation of Sidelobes

All of the codes considered so far have an equation for the code sequence, except for the Barker codes which are found by searching. Another way to generate codes is to start with an initial guess and then modify the code sequence in some way so as to minimise the sidelobe levels. One particular method transforms the code sequence to the autocorrelation series and back again whilst making small changes to the autocorrelation series to reduce the sidelobes and truncating the code sequence back to its required length and imposing any magnitude limits required [10]. The lower and upper magnitude limits can be set between 0 and 1. Setting both the lower and upper magnitude limits to 1 produces a CMC. Typically the lower limit is set to limit the power loss in the transmitted signal. For example setting the lower magnitude limit to 0.707 limits the transmitted power loss to 3dB. This algorithm will only converge to a local minimum, but can still produce good results. Figure 20 shows an example of an optimised code of length $N = 20$ with lower and upper magnitude limits set respectively to 0.5 and 1.0, which has a PSL of –30 dB below the mainlobe. Figure 21 of the radar ambiguity function shows that while the mainlobe is fairly constant over the extent of relative Doppler frequencies the sidelobes become much higher when $|f_R| \geq 0.004$.

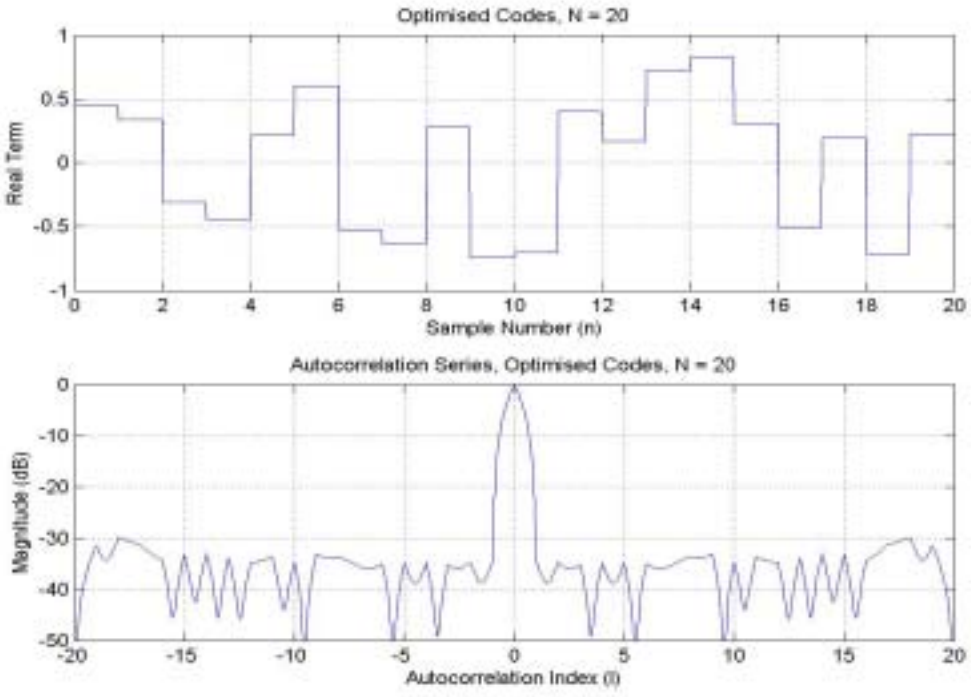

Figure 20. An Optimised Code and its Response Function

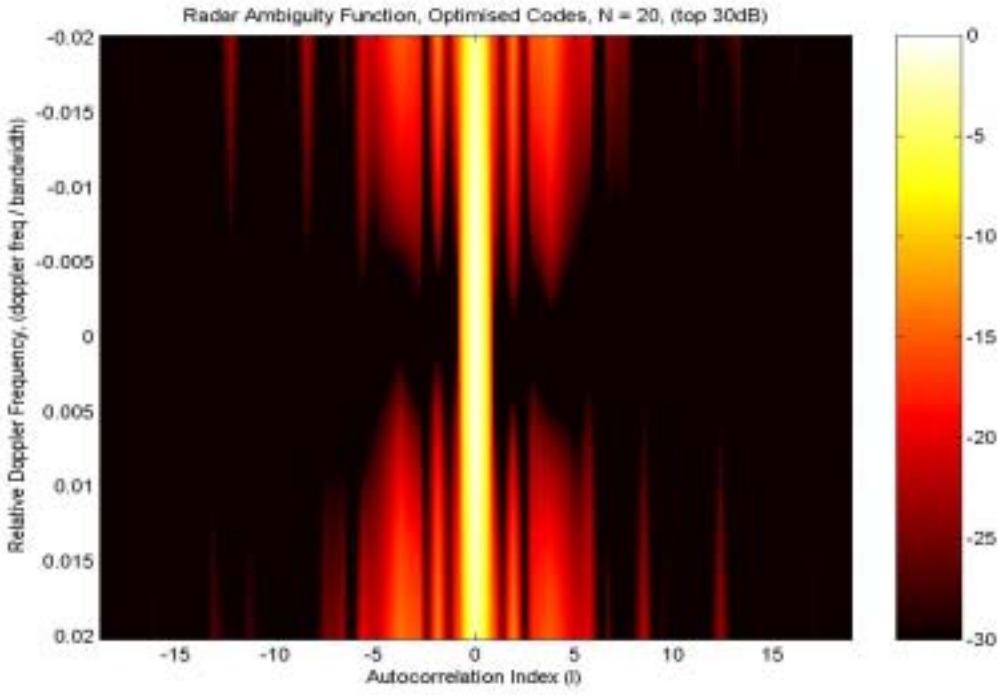

Figure 21. Radar Ambiguity Function for an Optimised Code

2.7 Mismatched Pulse Compression Filters

An option for reducing the PSL for cases where a small drop (usually 2dB or less) in the SNR can be tolerated is to use a mismatched pulse compression filter (MPCF). Given a code sequence that is to be transmitted by the radar it is possible using linear algebra to find a mismatched filter that minimises the integrated sidelobe level (ISL) (NB: the ISL is the sum of the magnitudes of all the sidelobes). An iterative algorithm can then be used to minimise the PSL, although this is not guaranteed to be the global minimum of the PSL [13].

This same method can be used on a pulse train to minimise both the autocorrelation series sidelobes of individual codes and the sidelobes of the crosscorrelation series between codes. Although this may be helpful our aim is to minimise the PSL in the range Doppler map.

Figure 22 shows the results for a primitive root code with a mismatched filter. Comparing this to the matched filter case (Figure 16) we see that by using a mismatched filter the PSL has fallen to –20 dB compared to –12 dB.

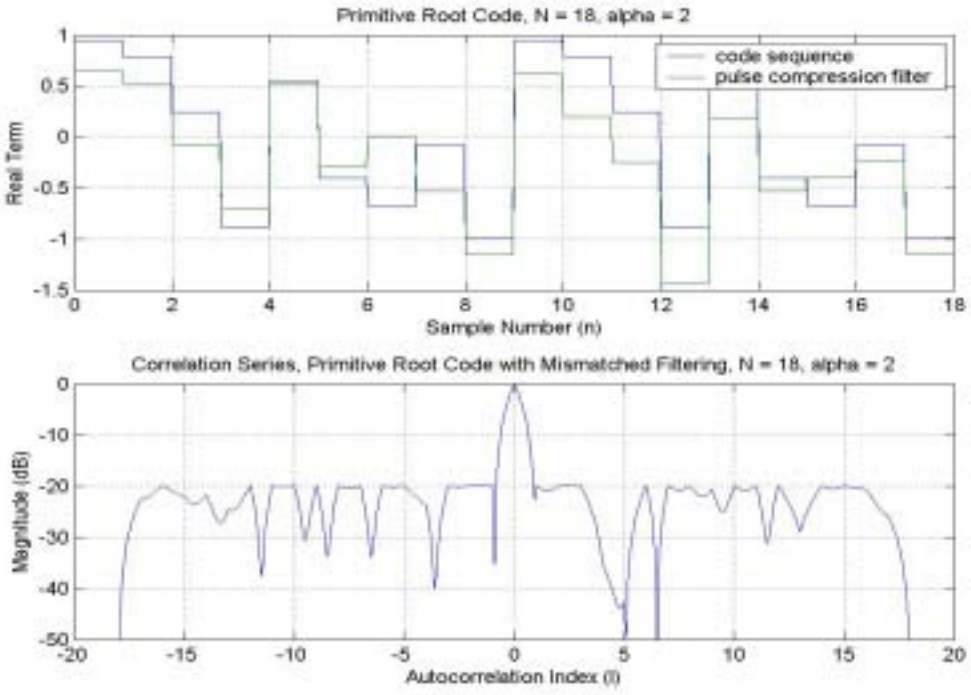

Figure 22. Primitive Root Code with Mismatched Filter

3. Pulse Trains

To produce a range Doppler map a radar transmits a number of pulses P with a fixed relatively long time delay between them. The received signals are arranged in a matrix where range bin number is the column and pulse number is the row. Pulse compression using matched filtering is applied to each row and then Doppler processing is applied down each column resulting in a range Doppler map.

The transmitted pulses are usually all the same waveform, because then any phase changes from pulse to pulse are due to Doppler returns. The case considered here is when the pulses have different waveforms pulse to pulse. This leads to pulse to pulse phase changes in the received signal that are due to the waveforms themselves and so the performance of the range Doppler radar can be degraded. The waveforms must vary pulse to pulse in an unpredictable way so that an enemy jammer cannot predict which waveform is coming next.

The main performance criterions are the PSL in the range Doppler map and the PJL of a jammer that is repeatedly transmitting one of the waveforms at the correct pulse repetition frequency (PRF).

Many schemes can be imagined for generating a pulse train of different waveforms. We have decided to initially only consider pulse trains where the different waveforms come from the same family of waveforms.

3.1 Generating Pulse Trains

3.1.1 Shifted Sampled Linear Chirp Pulse Trains

By slightly modifying the definition of the sampled linear chirp code we get,

$$a_{q,n} = \exp(j\frac{\pi(n+q)^2}{N}), n = 0,1,2,\ldots,N-1$$

where by setting q to any integer between 0 and $N-1$ a different code sequence will be generated. The code sequences can then be weighted or not weighted. These different code sequences are then transmitted in a random order to form a pulse train.

3.1.2 Shifted Frank Code Pulse Trains

By slightly modifying the definition of a Frank code we get,

$$a_{q,n} = \exp(j2\pi\frac{rkm}{M})$$

where,

$$m = \text{int}\left(\frac{n-q}{M}\right)$$

$$k = n - q - mM$$

r is chosen to be co-prime with M (i.e. no common factors between r and M), $1 \le r < M$ and the integer $M = \sqrt{N}$. Setting q to be an integer between 0 and $N-1$ generates different code sequences. These different code sequences are then transmitted in a random order to form a pulse train.

3.1.3 Binary Barker Code Pulse Trains

From Table 1 we see that for each code length for which BBCs exist there is a choice of at least four different BBCs. These can be transmitted in a random order to form a pulse train of any length. In all cases the number of different codes is only four to eight which is not ideal because an enemy jammer could potentially record all of these codes and retransmit them.

3.1.4 Barker on Barker Code Pulse Trains

For BBCs at least four codes exist for each valid length and so the number of different BoBCs that can be generated is at least 16. These can be transmitted in a random order to form a pulse train of any length.

3.1.5 Pseudo Noise Code Pulse Trains

From Table 2 we see that for code sequences of length 31 or greater there are at least three different feedback stage connections that can be used, furthermore the initial state of the shift register can be set to anything other than all zeros and so there will be numerous pseudo noise codes that can be generated. Although it must be pointed out that changing the initial state of the shift register whilst leaving the feedback stage connections the same will only vary the start point in the pseudo noise code. These can be transmitted in a random order to form a pulse train.

3.1.6 Primitive Root Code Pulse Trains

From Table 3 we see that for most valid values of the code length N there are a number of different primitive roots that can be used to generate different codes. These can be transmitted in a random order to form a pulse train.

3.1.7 Optimised Code Pulse Trains

The number of different optimised codes available will depend on the number of different local minimums in the optimisation problem. We have not investigated the number of different codes that can be found in this way but we suspect it would be large. A pulse train can then be generated by randomly ordering the required number of these.

It is important here to stress that here we are only considering codes that have been individually optimised. Another option is to optimise a whole pulse train concurrently to minimise the sidelobes in the range Doppler map. This case may be investigated at a later date.

3.2 Determination of the PSLs

The PSL is determined by setting the received signal to be equal to the transmitted pulse train. If the relative Doppler frequency f_R is not zero then a modulation of f_R is applied to each of the received pulses. The received signal is then processed into a range Doppler response function using Equation 1 and the largest sidelobe is found and normalised to the mainlobe. This is done 10 times to allow for different realisations of the pulse trains and the average PSL is found.

The standard deviations were estimated for each pulse train type and each code length N, Table 4 gives the largest standard deviations for each pulse train type.

Figures 23, 24 and 25 show the case where the relative frequency f_R is allowed to vary from –0.001 to +0.001, for the number of pulses $P = 10,20,30$ respectively. It is clear that for these three cases the two optimised codes have the lowest sidelobes, with sidelobes around –35dB for $P = 30$. The primitive root codes are the next best performer. Note how the sidelobes for the linear chirps and the Frank code rise with increasing code length N. This indicates that they are sensitive to the mismatch caused by the relative Doppler frequency f_R because as the code length N is increased the phase change across the code due to the Doppler shift becomes greater and so the sidelobes can become greater as the code length N is increased.

Figures 26, 27, and 28 are the same except that the relative frequency f_R is allowed to vary from –0.005 to +0.005. In these three cases all of the codes are very sensitive to the mismatch caused by the relative frequency f_R. The best performers are the optimised codes and the primitive root codes. But overall the performance is poor and so we conclude that allowing a relative Doppler frequency range of f_R equal to –0.005 to +0.005 is too large. This limits these waveforms to the case where the Doppler frequencies are low, or to the case where multiple pulse compression filters each matched to a different Doppler frequency are used.

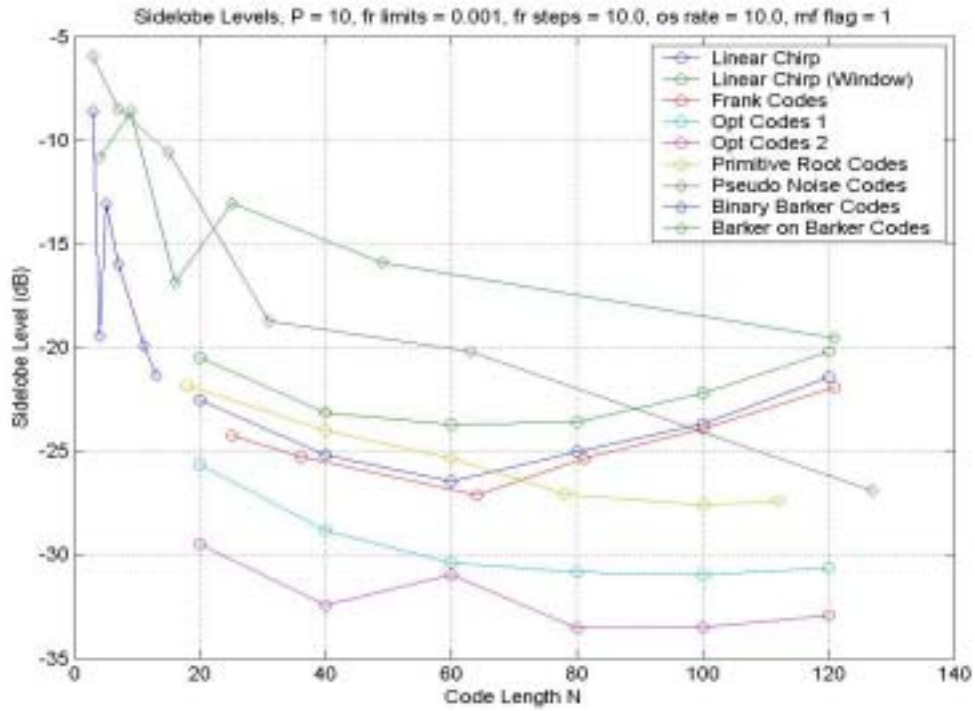

Figure 23. PSL in the Range-Doppler Map, ($P = 10$, $f_r = -0.001 \rightarrow 0.001$)

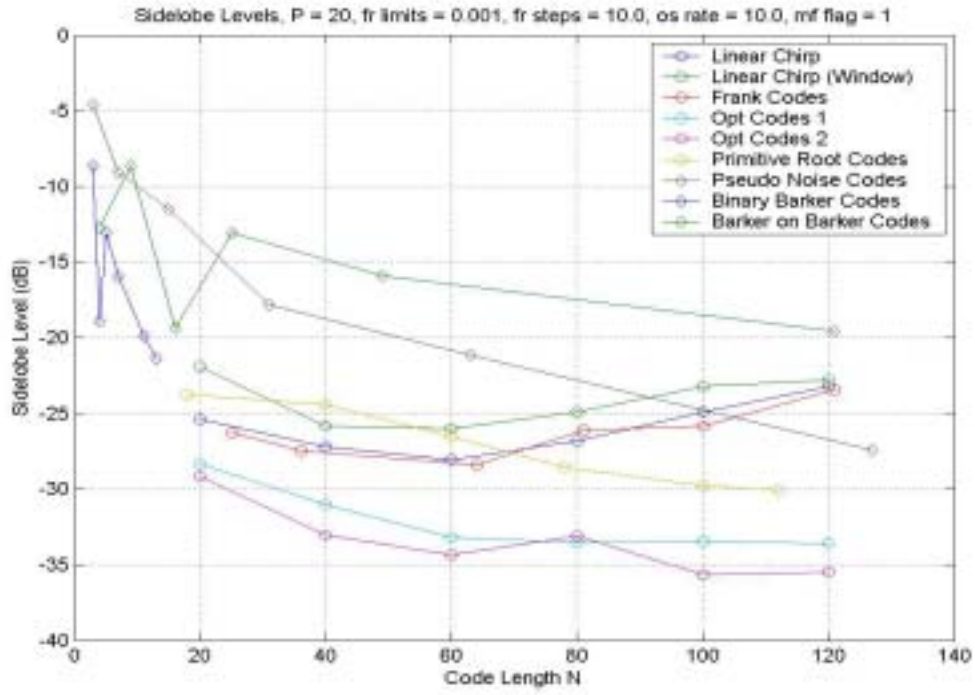

Figure 24. PSL in the Range-Doppler Map, ($P = 20$, $f_r = -0.001 \rightarrow 0.001$)

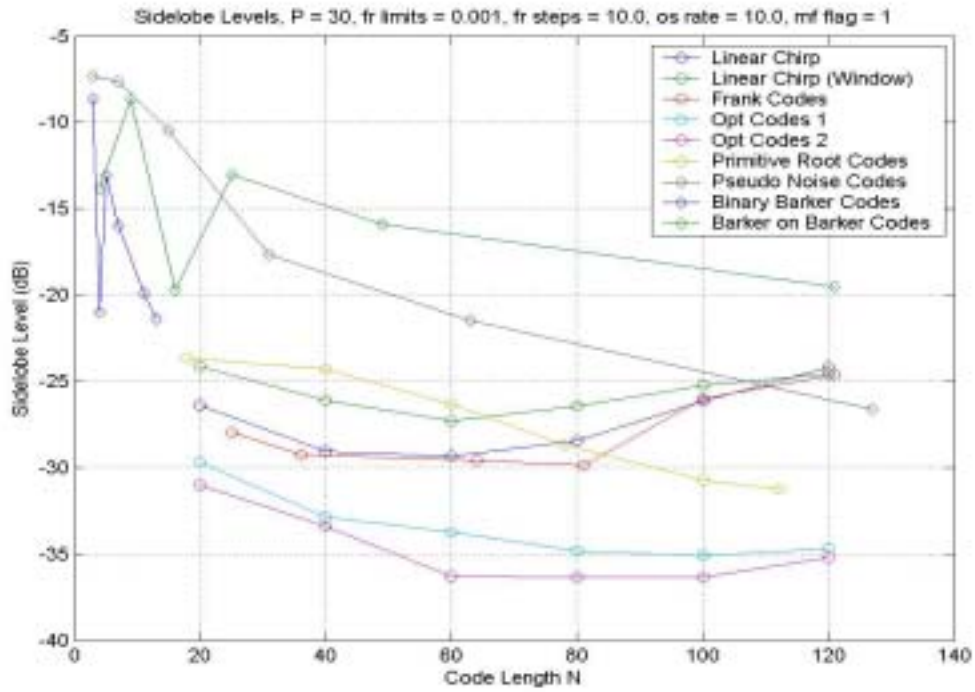

Figure 25. PSL in the Range-Doppler Map, ($P = 30$, $f_r = -0.001 \rightarrow 0.001$)

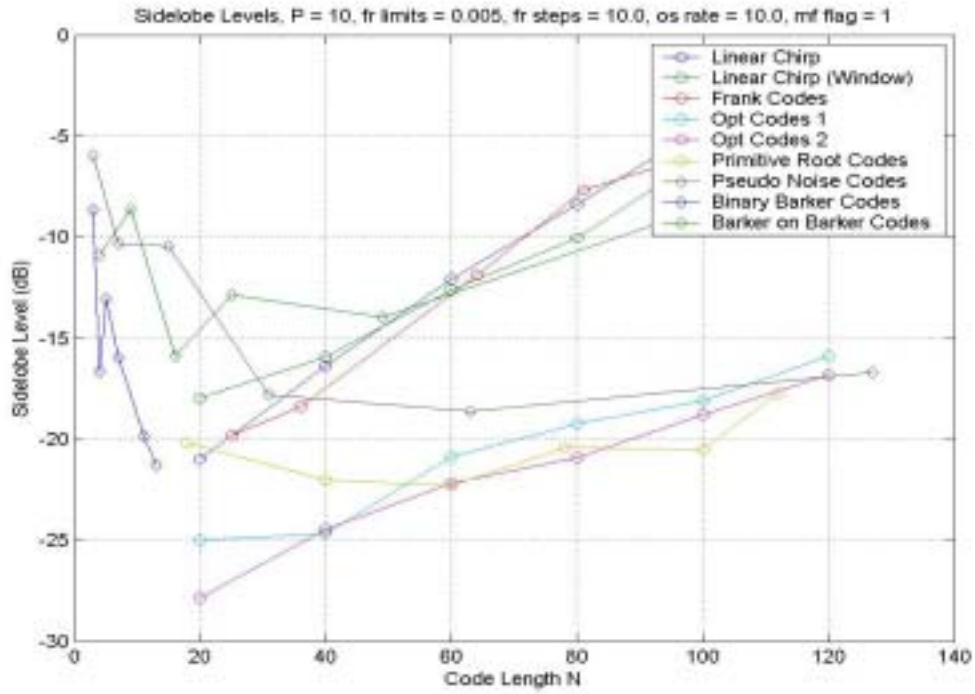

Figure 26. PSL in the Range-Doppler Map, ($P = 10$, $f_r = -0.005 \rightarrow 0.005$)

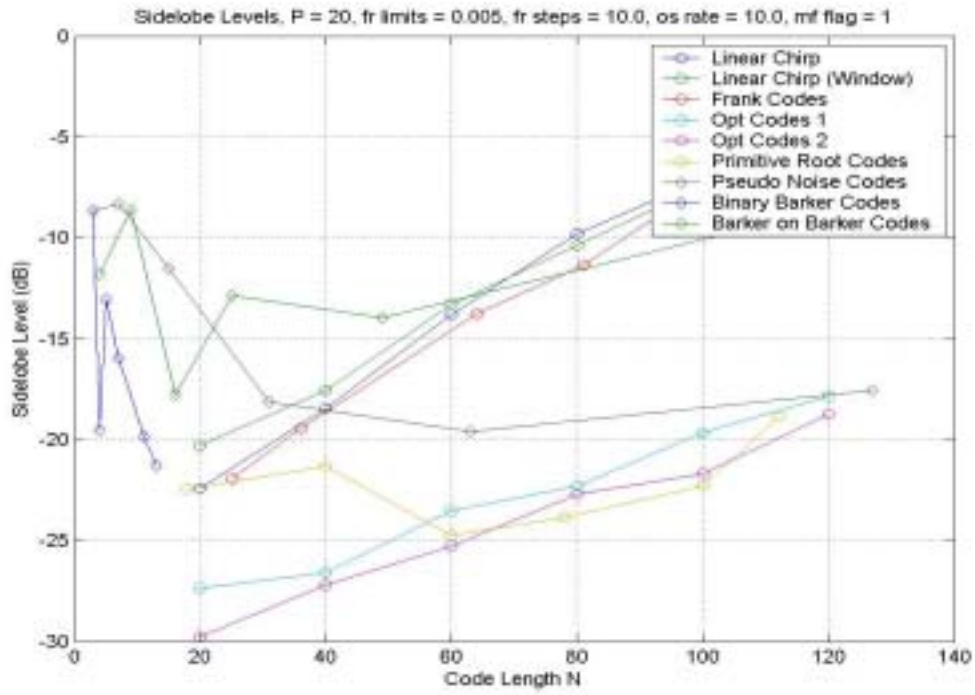

Figure 27. PSL in the Range-Doppler Map, ($P = 20$, $f_r = -0.005 \rightarrow 0.005$)

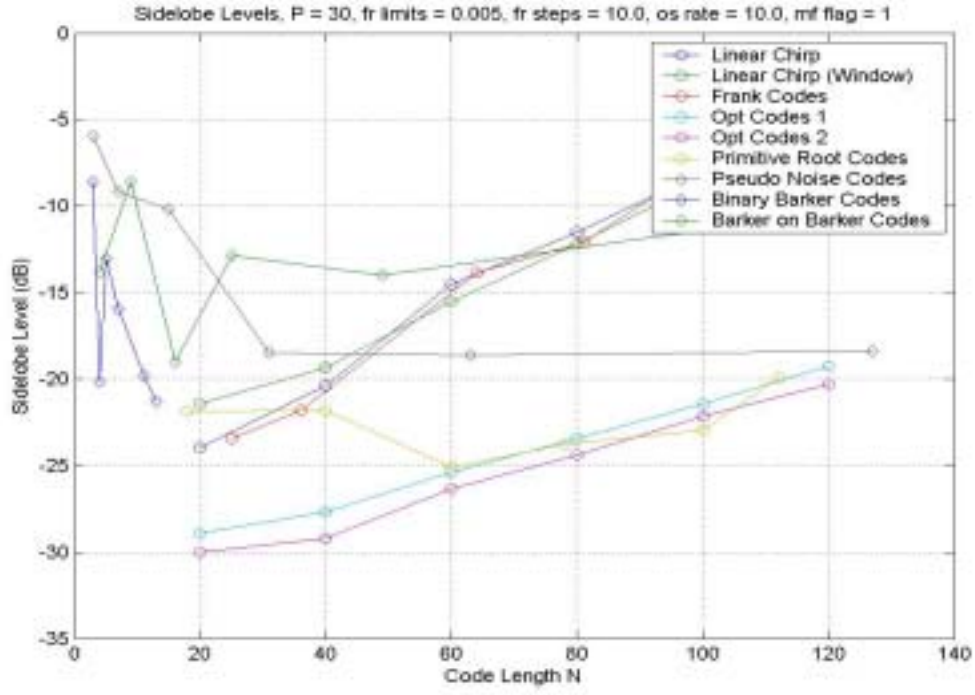

Figure 28. PSL in the Range-Doppler Map, ($P = 30$, $f_r = -0.005 \rightarrow 0.005$)

Table 4. Maximum Standard Deviation (dB) of the PSL

waveform	relative frequency limit = -0.001 to 0.001			relative frequency limit = -0.005 to 0.005		
	P = 10	P = 20	P = 30	P = 10	P = 20	P = 30
linear chirp	1.7	1.8	1.4	1.9	1.6	1.4
linear chirp (windowed)	1.8	1.6	1.3	5.5	1.7	1.5
Frank code	1.8	1.8	1.3	2.1	1.2	1.5
opt codes 1	1.0	0.8	1.1	1.1	1.2	1.0
opt codes 2	2.4	1.8	1.4	1.3	1.0	1.0
primitive root code	0.7	0.8	0.6	1.1	0.9	0.4
pseudo noise codes	3.7	3.0	3.0	4.2	1.9	4.0
binary Barker codes	0.0	0.0	0.0	0.0	0.0	0.0
Barker on Barker codes	1.1	1.0	1.2	1.0	1.5	1.0

3.3 Determination of the PJLs

The PJL is determined by forming the received signal by repeating the first waveform P times . This simulates a jammer that records the first pulse and repeats it to form a jamming waveform, (i.e. a coherent noise technique). The relative Doppler frequency f_R need not be taken into account because the worst case occurs when f_R is zero. The received signal is then processed into a range Doppler map and the largest peak is found and normalised to the mainlobe for the target only case. This is done several times to allow for different realisations of the pulse trains and the average PJL is found.

Table 5 gives the maximum standard deviations of the PSL for the cases shown in Figures 29, 30 and 31.

Figures 29, 30 and 31 show the PJLs respectively for the cases $P = 10,20,30$. In all three cases the linear chirps and the Frank codes have the lowest PJL values with PJL values of –28dB for $P = 30$. The optimised codes were the next best with PJL values about 5dB higher.

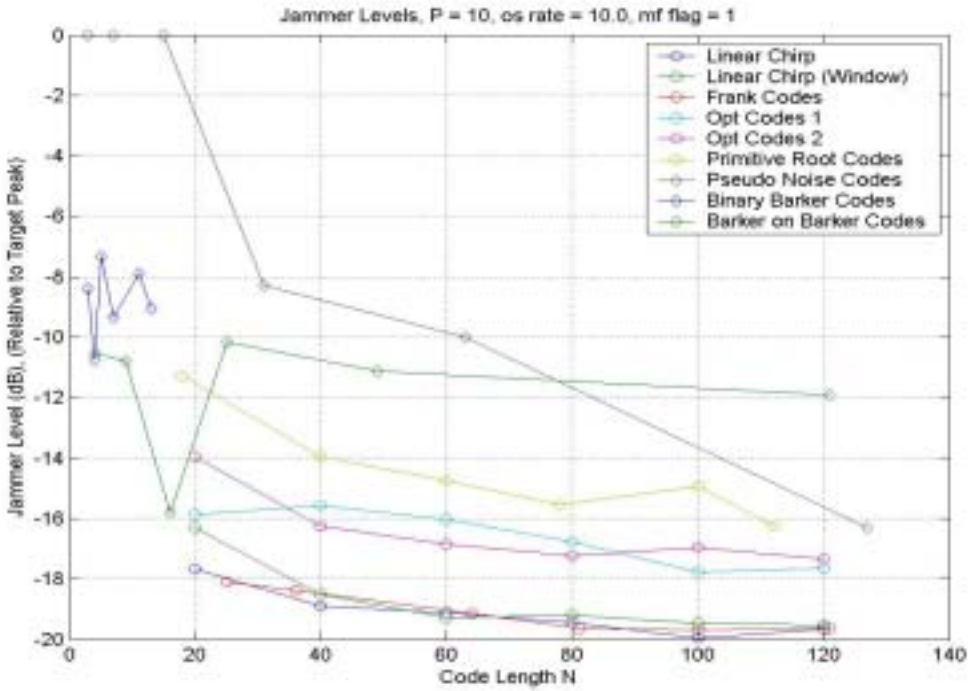

Figure 29. PJL in the range Doppler map, ($P = 10$)

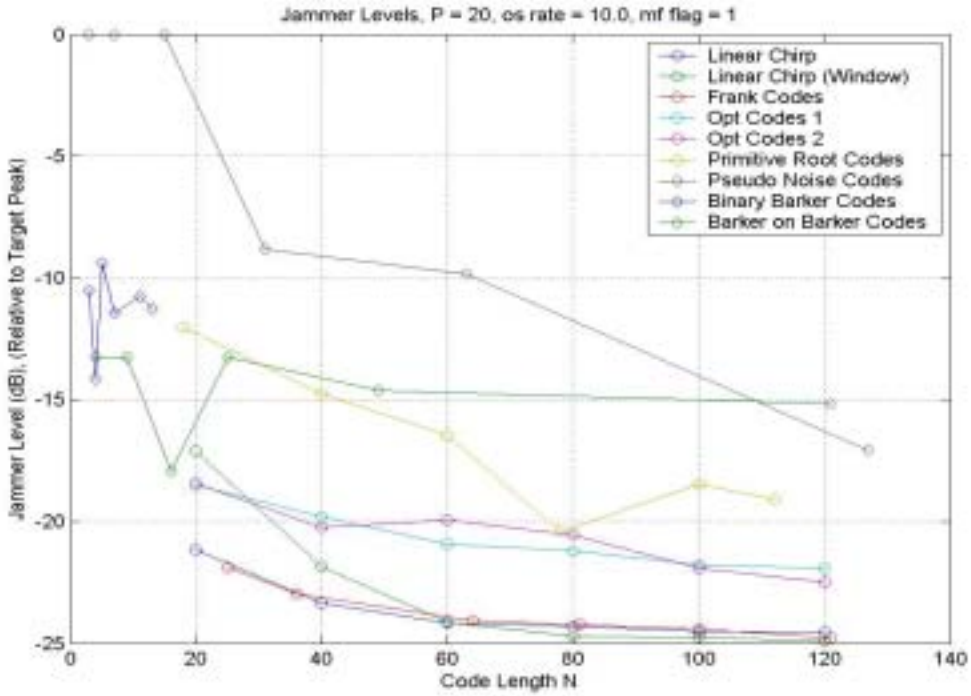

Figure 30. PJL in the range Doppler map, ($P = 20$)

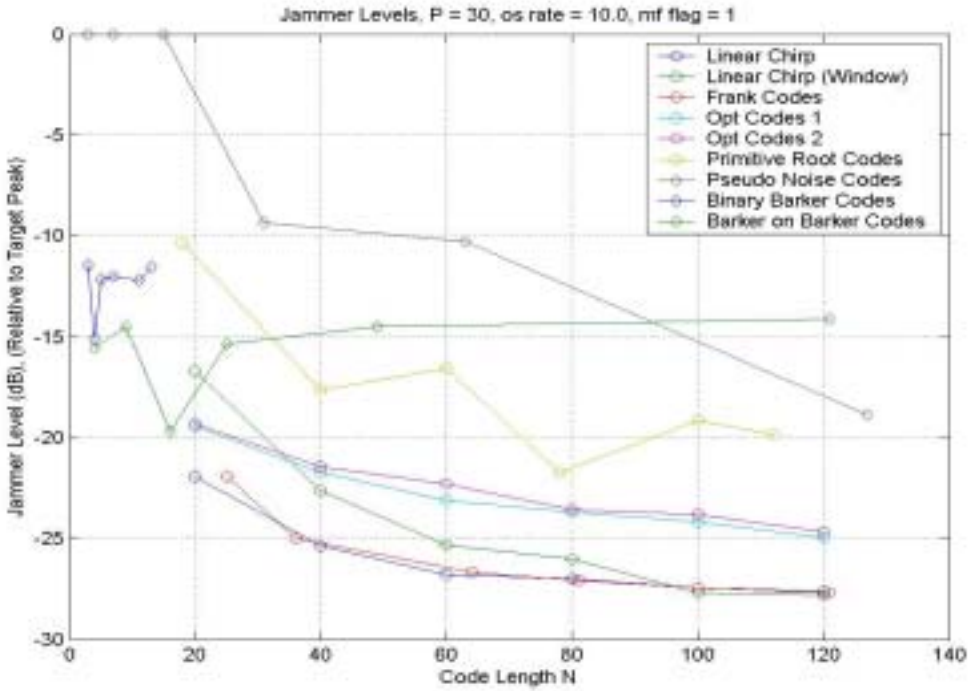

Figure 31. PJL in the range Doppler map, ($P = 30$)

Table 5. Maximum Standard Deviation (dB) of the PJL

waveform	relative frequency limit = -0.001 to 0.001			relative frequency limit = -0.005 to 0.005		
	P = 10	P = 20	P = 30	P = 10	P = 20	P = 30
linear chirp	0.3	0.5	0.4	0.5	0.3	0.5
linear chirp (windowed)	1.2	1.7	1.6	1.1	1.5	1.8
Frank code	0.35	0.5	0.6	0.3	0.5	0.5
opt codes 1	1.2	1.1	1.4	1.2	0.9	1.2
opt codes 2	1.1	1.0	1.4	1.1	1.3	1.3
primitive root code	2.0	2.0	1.2	1.5	2.2	1.4
pseudo noise codes	2.5	1.7	2.0	2.1	1.8	2.0
binary Barker codes	1.6	2.0	1.3	2.1	1.8	2.0
Barker on Barker codes	2.5	1.5	1.3	2.2	1.8	2.0

4. Conclusions and Future Directions

We have shown that the relative Doppler frequency limits must be –0.001 to +0.001 or less. For a bandwidth B of 1MHz this relates to a Doppler shift of 1kHz, which is a fairly low Doppler shift. For cases where the relative Doppler frequency varies by more than this a bank of pulse compression filters would be required.

For the case where the relative Doppler frequency varies over –0.001 to +0.001 the optimised codes were the overall best performers with a PSL of around –35 dB for P = 30 and N = 20 to 120 and a PJL equal to –19 dB to –25 dB for P = 30 and N = 20 to 120.

For a fixed waveform case a PSL of –40 dB is readily achievable, but the PJL would be 0dB since for the fixed waveform case there is no jammer rejection. Therefore a 25 dB improvement of the PJL has been achieved with only 5 dB degradation in the PSL. A 25 dB drop in PJL is equivalent to increasing the distance to the jammer by a factor of 17, so a jammer that has a range of 100 km for a fixed waveform radar will need to close to a range of 6 km for an waveform agile radar to achieve similar jamming results. The smaller jammer range will greatly increase the region in which the radar can operate effectively resulting in a strategic advantage.

Future research is to be carried out in the areas of the effect of Doppler processing on windowed waveforms (including the non linear chirp), complimentary waveforms and optimised pulse trains.

Windowed waveforms and non-linear chirps have main peaks that extend over more than one range bin. During Doppler processing the return is spread wide in Doppler and so the main peak is split, resulting in a very high PSL. The splitting of the peak will be investigated because if this can be resolved it will most likely result in a PSL value considerably lower than the –35 dB achieved here.

Complimentary waveforms consist of two or more waveforms that have autocorrelation series that sum to zero for all non-zero lags. These waveforms can be transmitted separated in time, frequency or polarisation. The performance of complimentary waveforms will be determined for the moving target case and methods of generating large numbers of sets of waveforms suitable for waveform agility will be determined.

Generation of pulse trains using an optimisation of the PSL and PJL will be undertaken, as this has the potential to achieve the lowest possible PSL and PJL values.

5. Bibliography

[1] D. Wehner, "High Resolution Radar", Artech House, 1987.

[2] Kretschemer and Gerlach, "New Pulse Compression Waveforms", 1988 IEEE Radar Conference, pp 194-198.

[3] M. Skolnik, "Radar Handbook", McGraw-Hill, 1991.

[4] R. Frank, "Polyphase Codes with Good Nonperiodic Correlation Properties, IEEE Transactions on Information Theory, pp. 43-45, 1963.

[5] Popovic, "Efficient Matched Filter for the Generalised Chirp Like Polyphase Sequences", IEEE Transactions on Aerospace and Electronic Systems, Vol. 30, No. 3, July 1994.

[6] Kretschemer and Gerlach, "Low Sidelobe Radar Waveforms Derived from Orthogonal Matricies", IEEE Transactions on Aerospace and Electronic Systems, Vol. 27, No. 1, January 1991.

[7] T. Felhauer, "New Class of Polyphase Pulse Compression Code with Unique Characteristics", Electronic Letters, Vol. 28, No. 8, 9th April 1992.

[8] R. L Frank, "Polyphase Complementary Codes", IEEE Transactions on Information Theory, Vol. IT-26, No. 6, November 1980.

[9] W. D. Wirth, "Compression of Polyphase Codes with Doppler Shift", FGAN-FFM, Germany, pp. 469-472.

[10] Bomer and Antweiler, "Polyphase Barker Sequences", Electronic Letters, Vol. 25, No. 23, 9th November 1989.

[11] New Wave Instruments, www.newwaveinstruments.com

[12] F. Kretschmer and K. Gerlach, "New Radar Pulse Compression Waveforms", 1988 IEEE Radar Conference, pp. 194.

[13] K. Griep, J. Ritcey and J. Burlingame, "Poly-Phase Codes and Optimal Filters for Multiple User Ranging", IEEE Transactions on Aerospace and Electronic Systems, Vol. 31, No. 2, April 1995.

DISTRIBUTION LIST

Preliminary Report on Pulse Compression Waveforms and their Application to Waveform Agility

Graeme Nash

AUSTRALIA

DEFENCE ORGANISATION

	No. of copies
Task Sponsor	
S&T Program	
Chief Defence Scientist	Shared
FAS Science Policy	
AS Science Corporate Management	
Director General Science Policy Development	
Counsellor Defence Science, London	Doc Data Sheet
Counsellor Defence Science, Washington	Doc Data Sheet
Scientific Adviser to MRDC, Thailand	Doc Data Sheet
Scientific Adviser Joint	1
Navy Scientific Adviser	Doc Data Sheet & Dist List
Scientific Adviser – Army	Doc Data Sheet & Dist List
Air Force Scientific Adviser	Doc Data Sheet & Dist List
Scientific Adviser to the DMO M&A	Doc Data Sheet & Dist List
Scientific Adviser to the DMO ELL	Doc Data Sheet & Dist List
Systems Sciences Laboratory	
Chief of Weapons Systems Division	Doc Data Sht & Dist List
Research Leader Land Weapons Systems	1
Research Leader Air Weapons Systems	1
Head RF Seekers	1
Dr Graeme Nash	1
Chief Electronic Warfare and Radar Division	1
Research Leader Microwave Radar	1
Head Airborne Radar	1
Head Phased Array Radar	1
Head Maritime Radar	1
DSTO Library and Archives	
Library Fishermans Bend	Doc Data Sheet
Library Edinburgh	1
Defence Archives	1

Capability Development Group

Director General Maritime Development	Doc Data Sheet
Director General Capability and Plans	Doc Data Sheet
Assistant Secretary Investment Analysis	Doc Data Sheet
Director Capability Plans and Programming	Doc Data Sheet
Director Trials	Doc Data Sheet

Chief Information Officer Group

Deputy CIO	Doc Data Sheet
Director General Information Policy and Plans	Doc Data Sheet
AS Information Strategy and Futures	Doc Data Sheet
AS Information Architecture and Management	Doc Data Sheet
Director General Australian Defence Simulation Office	Doc Data Sheet
Director General Information Services	Doc Data Sheet

Strategy Group

Director General Military Strategy	Doc Data Sheet
Director General Preparedness	Doc Data Sheet
Assistant Secretary Strategic Policy	Doc Data Sheet
Assistant Secretary Governance and Counter-Proliferation	Doc Data Sheet

Navy

SO (SCIENCE), COMAUSNAVSURFGRP, NSW	Doc Data Sht & Dist List
Maritime Operational Analysis Centre, Building 89/90 Garden Island Sydney NSW	Doc Data Sht & Dist List
Deputy Director (Operations)	
Deputy Director (Analysis)	
Director General Navy Capability, Performance and Plans, Navy Headquarters	Doc Data Sheet
Director General Navy Strategic Policy and Futures, Navy Headquarters	Doc Data Sheet

Air Force

SO (Science) - Headquarters Air Combat Group, RAAF Base, Williamtown NSW 2314	Doc Data Sht & Exec Summ

Army

ABCA National Standardisation Officer	e-mailed Doc Data Sheet
Land Warfare Development Sector, Puckapunyal	
SO (Science) - Land Headquarters (LHQ), Victoria Barracks NSW	Doc Data & Exec Summary
SO (Science), Deployable Joint Force Headquarters (DJFHQ) (L), Enoggera QLD	Doc Data Sheet

Joint Operations Command

Director General Joint Operations	Doc Data Sheet
Chief of Staff Headquarters Joint Operations Command	Doc Data Sheet
Commandant ADF Warfare Centre	Doc Data Sheet
Director General Strategic Logistics	Doc Data Sheet

Intelligence and Security Group

DGSTA Defence Intelligence Organisation	1
Manager, Information Centre, Defence Intelligence Organisation	1 (PDF)
Assistant Secretary Capability Provisioning	Doc Data Sheet
Assistant Secretary Capability and Systems	Doc Data Sheet
Assistant Secretary Corporate, Defence Imagery and Geospatial Organisation	Doc Data Sheet

Defence Materiel Organisation

Deputy CEO	Doc Data Sheet
Head Aerospace Systems Division	Doc Data Sheet
Head Maritime Systems Division	Doc Data Sheet
Chief Joint Logistics Command	Doc Data Sheet

Defence Libraries

Library Manager, DLS-Canberra	1
Library Manager, DLS - Sydney West	Doc Data Sheet

OTHER ORGANISATIONS

National Library of Australia	1
NASA (Canberra)	1
Library of New South Wales	1

UNIVERSITIES AND COLLEGES

Australian Defence Force Academy

Library	1
Head of Aerospace and Mechanical Engineering	1
Serials Section (M list), Deakin University Library, Geelong, VIC	1
Hargrave Library, Monash University	Doc Data Sheet
Librarian, Flinders University	1

OUTSIDE AUSTRALIA

INTERNATIONAL DEFENCE INFORMATION CENTRES

US Defense Technical Information Center	2
UK Dstl Knowledge Services	2
Canada Defence Research Directorate R&D Knowledge & Information Management (DRDKIM)	1
NZ Defence Information Centre	1

ABSTRACTING AND INFORMATION ORGANISATIONS

Library, Chemical Abstracts Reference Service	1
Engineering Societies Library, US	1
Materials Information, Cambridge Scientific Abstracts, US	1
Documents Librarian, The Center for Research Libraries, US	1

INFORMATION EXCHANGE AGREEMENT PARTNERS

National Aerospace Laboratory, Japan	1
National Aerospace Laboratory, Netherlands	1
SPARES	5
Total number of copies: Printed: 39 PDF: 1	**40**

DEFENCE SCIENCE AND TECHNOLOGY ORGANISATION
DOCUMENT CONTROL DATA

1. PRIVACY MARKING/CAVEAT (OF DOCUMENT)

2. TITLE

Preliminary Report on Pulse Compression Waveforms and their Application to Waveform Agility

3. SECURITY CLASSIFICATION (FOR UNCLASSIFIED REPORTS THAT ARE LIMITED RELEASE USE (L) NEXT TO DOCUMENT CLASSIFICATION)

Document	(U)
Title	(U)
Abstract	(U)

4. AUTHOR(S)

Graeme Nash

5. CORPORATE AUTHOR

Systems Sciences Laboratory
PO Box 1500
Edinburgh South Australia 5111 Australia

6a. DSTO NUMBER	6b. AR NUMBER	6c. TYPE OF REPORT	7. DOCUMENT DATE
DSTO-TR-1631	AR-013-212	Technical Report	October 2004

8. FILE NUMBER	9. TASK NUMBER	10. TASK SPONSOR	11. NO. OF PAGES	12. NO. OF REFERENCES
2004/1046972/1	04/059	DGMD	34	13

13. URL on the World Wide Web

http://www.dsto.defence.gov.au/corporate/reports/DSTO-TR-1631.pdf

14. RELEASE AUTHORITY

Chief, Weapons Systems Division

15. SECONDARY RELEASE STATEMENT OF THIS DOCUMENT

Approved for public release

OVERSEAS ENQUIRIES OUTSIDE STATED LIMITATIONS SHOULD BE REFERRED THROUGH DOCUMENT EXCHANGE, PO BOX 1500, EDINBURGH, SA 5111

16. DELIBERATE ANNOUNCEMENT

No Limitations

17. CITATION IN OTHER DOCUMENTS Yes

18. DEFTEST DESCRIPTORS

Radars; Jammers; Radiofrequency; Waveforms

19. ABSTRACT

Pulse Doppler radars predominantly transmit the same pulse compression waveform pulse to pulse. This produces good Doppler performance in a jammer free environment. But in a jammer environment the transmitted pulses can be captured by a digital RF memory (DRFM) and retransmitted creating false targets. By introducing pulse to pulse waveform agility the effectiveness of the jammer can be greatly reduced.